

Interactive comment on “Continental pollution in the Western Mediterranean Basin: vertical profiles of aerosol and trace gases measured over the sea during TRAQA 2012 and SAFMED 2013” by C. Di Biagio et al.

At first, we would like to thank the reviewers for having carefully read the paper and provided valuable comments which helped to improve the quality of the manuscript. We have taken into consideration all the questions raised by the reviewers, and changed the paper accordingly. The details of our changes are highlighted in the text. The point by point answers to Reviewer #1 and #2 are provided in the following.

Anonymous Referee #1

Received and published: 16 April 2015

The paper focuses on the analysis of aerosol and trace gas vertical profiles obtained over the sea in the Western Mediterranean Basin during the TRAQA 2012 and SAFMED 2013 summer campaigns. Even though the number of measurements presented in this paper is relatively short (23 profiles), it reasonably covers large area in the western Mediterranean basin providing insight of the impact of the different pollution transport regimes.

I have some suggestions for a minor revision of the manuscript (see below).

Specific comments

Abstract Lines 8-10 page 8285: this sentence is unclear. Maybe the authors mean that during TRAQA and SAFMED campaigns the study area was under a wide range of meteorological conditions that favored the pollution export from different sources located around the basin which allowed sampling atmospheric aerosols of different origin and types. Please, rephrase this sentence.

The abstract has been corrected as suggested by the reviewer.

Lines 13-15 page 8285: authors state that aerosol layers not specifically linked with Saharan dust outflows are distributed ubiquitously which indicates “quite elevated levels “of background pollution throughout the Western Basin. This statement is not justified by data analysis presented in this paper. Authors do not presented the analysis of background conditions over the study area. Please clarify this point and provide information that can justify these “quite elevated levels “of “background pollution”.

The sentence “Aerosol layers not specifically linked with Saharan dust outflows are distributed ubiquitously which indicates quite elevated levels of pollution throughout the Western basin” has been eliminated from the abstract. We agree that it is not precise.

Introduction The recently published papers by Valenzuela et al., 2014 and Lyamani et al., 2005 should be referred in this manuscript. Valenzuela et al., 2014. Aerosol transport over the western Mediterranean basin: Evidence of the contribution of fine particles to desert dust plumes over Alborán Island. Journal of Geophysical Research D: Atmospheres, 119 (24), pp. 14028-14044

Lyamani et al., 2015. Aerosol properties over the western Mediterranean basin: Temporal and spatial variability. *Atmospheric Chemistry and Physics*, 15 (5), pp. 2473-2486.

Despite their interesting results, these papers analyses data from a region quite far to our investigation area and much more under the influence of different meteorological/aerosol export conditions compared to those analysed in this study. For these reasons we have not included these two valuable papers in the references.

Lines 2-3 page 8288: Please correct by “During TRAQA and SAFMED the Western Basin was under diverse synoptic conditions”.

The correction has been made.

Line 4 page 8288: Please provide a brief description of Mistral/Tramontane events. This will help understand the interpretations of the results.

We have added a brief description of the Mistral/Tramontane in Section 4, when describing the different meteorological conditions: “On the same days a strong Mistral-Tramontane episode (i.e., strong northerly winds developing along the Rhône and Aude valley which bring a northerly/north-westerly flow over the Western Mediterranean, see Fig 3a) favoured the dispersion of pollutants towards the central part of the Western basin”.

Lines 7-8 page 8288: The authors state that the main objective of the present work is to provide “extensive observations” of the vertical distribution of aerosols and trace gases. However, they only present 23 profiles. Please, be precise.

The term “extensive” has been eliminated.

Section 3.2 Line 1 page 8293: between 0.1 and 3.0 μm or between 0.11 and 4.17 μm ? Please check.

The text is correct and is well 0.1-3.0 μm ; however we found a typos in page 8290 line 12 since the CPC range is 0.004-3.0 μm , instead of 0.004-1.0 μm as stated in the text. This has been corrected in the text.

Line 19 page 8294: eq. (2) instead eq. (1)

The correction has been made.

Section4. A brief description of the AERONET data (data level, accuracy of the data, etc.) and the instrument used should be provided. In addition, information on AERONET sites (characteristic, location, etc.) should be given. Please include these sites in Fig.1. This may help to make clear the interpretation of the results.

The first paragraph of Section 4 has been rewritten as: “In order to characterize the general aerosol conditions encountered over the Western Mediterranean basin during the TRAQA and the SAFMED campaigns we have plotted the time-series of the aerosol optical depth (τ , ± 0.02) at 440 nm and the 440-870 nm Ångström exponent (α) measured with a Cimel sunphotometer (Holben et al., 1998) at the three AERONET stations of Barcelona, Frioul, and Erso located along the coast around the Western basin (see Fig. 1). Level 1.5 cloud-screened data are used in this study.”

Fig. 1 has been also modified to include the 3 AERONET stations.

For the AERONET data I used the Level 1.5 for which data from all the stations were available. For the stations for which they were available, the comparison with Level 2.0 data does not indicate any difference in the interpretation of the results.

Lines 19-20 page 8295: it is obvious that TRAQA campaign in 2012 was characterized by very variable meteorological conditions than SAFMED campaign because TRAQA campaign period (20 June–13 July 2012) was larger than SAFMED campaign period (24 July–1 August 2013). On the other hand, I don't understand how very variable meteorological conditions can prevent the accumulation of high levels of pollutants over the basin. Some meteorological conditions as discussed later by the authors were responsible of high pollution events during TRAQA campaign. Please clarify and rephrase this sentence.

The sentence “The TRAQA campaign in 2012 was characterized by very variable meteorological conditions which prevented the accumulation of high levels of pollutants over the basin” was probably speculative. The whole sentence has been eliminated from the text.

The title (“Events observed”) of the last column of table 1 is not adequate. For example “Test flight” , “Follow of Barcelona pollution plumes “ and “Characterization of pollution in central Italy” are activities that have been carried out and not events that were observed during these campaigns. Please correct.

The column title has been changed in “Description”.

Line 15 page 8295: authors state that Fig. 2 show data corresponding to the period of the campaign of measurements plus 10 days before and after. However, Barcelona data (left panels) correspond to the period of the campaign plus 1 day before and after. Please check.

Data for the Barcelona station are not available over the whole considered period in 2012. The caption of Figure 2 has been rewritten as: “Aerosol optical depth at 440 nm (τ) and Ångström exponent (α) measured at the Barcelona, Frioul, and Ersu AERONET stations during the TRAQA 2012 (left panels) and the SAFMED 2013 (right panels) campaigns. The time period for the different plots is ± 10 days around the beginning/end of the two campaigns (data for the Barcelona station are not available over the entire period for 2012). The label D indicates the days affected by Saharan dust”.

Lines 21-22 page 8295: the aerosol optical depth was below 0.2 before the beginning of the campaign over the three analyzed AERONET sites and not over the whole basin. Please be precise. In addition, authors sate that the aerosol optical depth (AOD) increased to 0.3–0.5 (with $1 < \alpha < 2$) in the periods 23–26 June and 3–13 July. However, as can be seen in Fig. 2 the aerosol optical depth was in general below 0.2 over the three AERONET sites during 23–26 June. Also, the AOD was in general below 0.3 (especially at Frioul and Ersu) during 3–13 July. However, from fig2, it can be seen that the aerosol optical depth was relatively high from 30 June to 4 July which was associated with dust intrusions. Please check and correct.

The sentence has been rewritten as: “Over the analysed AERONET sites the aerosol optical depth was below 0.2 before the beginning of the campaign and increased, especially at Barcelona and Ersu, to $\sim 0.3-0.5$ (with $1 < \alpha < 2$) in the periods 23-26 June and 3-13 July”.

For clarity please reduce the y-scale of fig.2.

The y-scales for the optical depth and Angstrom exponent have been reduced as much as possible.

The authors present Fig 3, but, don't discuss it. Please, discuss this figure or remove it from the paper because it does not add any significant information.

Figure 3 can be useful to identify the different meteorological conditions encountered during the campaign, as for example the Mistral/Tramontane event cited by the reviewer, so we decided to maintain this Figure. Reference to Fig. 3a and 3b has been made within the text of Section 4.

Lines 4-6 page 8296: Please, specify if this export regime has occurred at all altitude levels or at specific altitude. The same should be done for the other described export regimes. This is because export regime can be different at different altitudes.

The main objective in Section 4 is to provide an overview of the main different conditions encountered during the different flights, so to understand the general strategy and observed continental outflow regimes. A more detailed analysis of the different flights, including wind vertical profiles and back-trajectory analysis, is performed in Sect. 5. We do not think necessary to specify all the details here.

Lines 4-6 page 8296: authors state that on 26–27 June north/north-easterly winds blew across northern Italy determining an air mass outflow towards the Gulf of Genoa. However, Fig.9 shows that the air masses on 27 June come from France and not pass over Italy. Please check and correct.

We have checked and the text has been changed in north/north-westerly.

Lines 3-19 page 8296: Mediterranean Sea and ship traffic are important source contributing to the aerosol loading over the Mediterranean Sea. The authors cannot a-priori exclude this important sources.

Ship emissions are undoubtedly a very important source of pollution over the sea mostly close to the surface. During TRAQA and SAFMED flights covered an extended altitude range up to 5000-6000 m, so ship emissions can influence the profiles predominantly in the lowest atmospheric layers. A reference to the possible impact of ship emissions has been added in Sect. 5.4 in reference to flight V28 discussed there.

Line 12 page 8296. I think that authors refer to Fig 1 and not to Fig3. Please verify.

The correction has been made.

Lines 12-14 page 8296: this sentence seem to be not related to this section. To be consistent, authors should describe the meteorological/export during flight V31 as they did for the other flights. Please, explain what you mean with “moderate” Mistral episodes.

For V31 the sentence has been rewritten as: “Additionally, flight V31 sounded the atmospheric structure close to the Spanish coasts reaching the southern urban area of Valencia. The flight was performed under the influence of south-westerly winds favouring the export from the Iberian Peninsula towards the basin”.

The reviewer is correct and “moderate” is not necessary, so I rewrote as “(iv) Mistral episodes occurred on the 6-7 and 11 July 2012”.

5 Results Figure 5 is poorly discussed and interpreted. More discussion and interpretation of the results presented in this figure is needed. If no more discussion and interpretation of this figure is given this figure should be removed from the paper.

I understand that the reviewer does not consider Fig. 5 sufficiently discussed, however it represents the starting point of whole Section 5. The fact observing such variability in the scattering coefficient, particle concentration, and trace gases as shown in the figure is the key point that motivates the detailed investigation of the different flight observations. Moreover, Fig. 5 summarizes the range of observations encountered during the campaigns, so providing a reference for pollution conditions in the Western Mediterranean basin.

Section 5.1 The figures presented in fig.6 should have the same X and Y scales. Also, vertical profile of Angstrom exponent should be included in this figure. This in combination with dN_{Acc} and dN_{Coarse} will help to identify the type of aerosols dominant in each layer.

The x and y scales in Fig. 6 have been corrected. Conversely, for what concerns the Angstrom exponent, we have decided not to add it to the plot. We find that it does not add any further information to the plot. In fact, the information on the type of the particles is already given by the spectral variability of the scattering coefficient (pronounced spectral variability corresponds to small particles, so to a higher Angstrom exponent; a neutral spectral variability corresponds to large particles, so to a lower Angstrom exponent).

Finally, Fig. 6 already contains a large number of information and adding another parameter would reduce the clarity of the figure.

Scattering profiles during TRAQA campaign (6 s resolution) are noisier than those observed during SAFMED (1 s resolution). Please give an explanation for this.

The stronger noise during TRAQA is probably due to the non-perfect cleaning of the nephelometer cavity during this campaign compared to SAFMED, for which the nephelometer was cleaned before the beginning of the campaign. This effect however does not affect the interpretation of the results.

Lines 8-10 page 8298: authors state that the profile of the aerosol scattering coefficient is mostly correlated to dN_{Acc} , however, they not justify this statement. Please give statistical parameter that justifies this statement.

What we wanted to highlight in this section was the link between the particle concentration in the accumulation mode and the scattering coefficient, which is quite evident by looking at the plots, and not to estimate quantitatively this relation. In order to avoid any confusion on this point the text has been changed in “The structure in the scattering profile is generally mirrored in dN_{Acc} profile.”.

Lines 16-20 page 8298: Please, provide an explanation of the cause of scattering coefficient and dN_{Acc} maxima and minima.

As stated in the text the minima and maxima during SAFMED are associated to the different phases of the campaign, the first more polluted and the second one less polluted as discussed in Sect. 4.

Concerning TRAQA, the absolute maxima are obtained in correspondence of the dust event. Some details have been added in the text.

Lines 3-5 page 8299: authors state that the scattering coefficient and the particle concentration measured in the FT are comparable with the values observed in the BL, and in few cases even larger (V25, V26, V30). This contradicts with the results shown in fig. 5. Please check and correct.

This sentence refers to the fact that in single profiles the measured values of the scattering coefficient and particle concentration may be larger in the FT than in the BL, as it is observed in some profiles (see Fig. 6). The box and whisker plot, conversely, describe the entire dataset and gives an overview over all conditions. This point has been specified in the first paragraph of the Results Section.

Lines 16-19 page 8299: Please, include Table comparing your results with those found in literature. Also, for better comparison (same experimental set), authors should include their results obtained over land in this table (e.g. flight V49).

A new table (Table 2) has been added. This table resumes the measurements of dN_{Aitken} and dN_{Acc} in the BL and in the FT for the entire set of observations, also in comparison with literature data obtained over continental Europe. Data for V49 over land during SAFMED has not been added to the Table since no data are available for the CPC for the majority of this flight, so no information on dN_{Aitken} can be retrieved.

Lines 16-19 page 8299: during flights V52, the scattering coefficient was very low and no pollution aerosol layer can be seen in this flight as confirmed by authors. Authors should include a Table comparing the data obtained under the different main meteorological/export conditions. This will help to identify the main cause (and sources) of high pollution levels over Mediterranean Sea.

For TRAQA and SAFMED we measured different outflow conditions which can be useful to describe the complexity of the export towards the basin. However comparing data for the different cases would appear quite complicated. We consider that adding such a Table, as suggested by the reviewer, would require having a larger statistic of cases.

Section 5.2 Lines 26-28 page 8300: please give references that support your statement. Also, include Table comparing your results with those obtained during flight over land and with those found in literature.

As a support to my statement I have added the reference by Parrish et al. (1998) which define moderate pollution when $\text{CO} < 180$ ppbv. CO and O_3 have not been added in Table 2, however we have rewritten the first paragraph of Section 5.2 to take into account your suggestion: “CO and O_3 vary in the range 60-165 ppbv and 30-85 ppbv, respectively. The 25th and 75th percentiles are 87 and 105 ppbv for CO and 49 and 62 ppbv for O_3 , representative of moderate pollution conditions (Parrish et al., 1998). By comparison, the values measured over land in central Italy during flight V49 are in the range 80-180 ppbv for carbone monoxide and 40-85 ppbv for ozone”.

Section 5.3 Lines 11-13 page 8302: Please provide Table comparing your results with those reported by these authors.

We have added the values of the reference papers cited in parenthesis within the text of Section 5.3. The text has been rewritten as: “respectively, with a corresponding $\Delta O_3/\Delta CO$ ratio which varies in the range ~ 0.10 - 2.0 for all cases. These values are comparable with the range of observations available in the literature for fresh and moderately aged pollution plumes in the BL and in the lower FT (~ 0.2 - 1.0) (Chin et al., 1994; Parrish et al., 1998; Zhang et al., 2006; Cristofanelli et al., 2013)”.

Section 5.4. Line 24 page 8302: statistical analysis should be provided to justify the good correlation between dN_{Aitken} and dN_{Acc} , CO, and O₃. From Fig. 10 it can be seen that dN_{Aitken} and dN_{Acc} , CO, and O₃ are not correlated.

The text has been corrected and rewritten as: “For about half of the observed events the dN_{Aitken} layer appears related to a simultaneous increase in dN_{Acc} , CO, and O₃, which suggests that the layer has been transported from a region directly emitting in this size range”.

Lines 7-24 page 8305: I think that this dN_{Aitken} event can be simply associated to ship emissions.

We have rewritten the sentence as: “For the V28 layer (Fig. 10b) the dN_{Aitken} is correlated with CO which might indicate the influence of local emissions close to the surface level (i.e., ship emissions)”.

Conclusion

Lines 19-21 page 8307: authors state that the geographical distribution of aerosols and trace gases observed in this study appears quite homogeneous within the investigated area, suggesting a relatively similar contribution from the various sources located around the north-western basin. However, the results presented in this paper show that the aerosol and gas profiles obtained in different areas in the Mediterranean basin show very different structure and composition. Please clarify this point.

We agree with the reviewer and the entire sentence has been eliminated from the text.

Anonymous Referee #2

The manuscript presents airborne measurements of aerosols and trace gases CO and ozone over the Mediterranean focusing on the vertical distribution of several compounds within a series of vertical profiles between Spain, Corsica and the Gulf of Genova. Ozone and CO values respectively their ratio are used to characterize air masses. Such vertical distribution data over the Mediterranean are very scarce. They show that both Saharan dust and continental pollution are present in large amounts. Several of the compounds measured are not detectable from the ground or from remote sensing techniques although they are possibly crucial for the Mediterranean climate. It is highly recommended that such data are getting available.

However, the manuscript has several weaknesses that need some further work especially in the detailed description of the individual profiles. Generally the graphics of Fig. 6, 8 and 10 lack the size and resolution required. Within the text often a series of profiles are mentioned. For the reader it's difficult to find these profile data without having an indication in which of the different figures

these data are contained. Some figures are labelled a or b without having a description in the text. For example V28 in Fig. 10 looks different from V28b in Fig. 6.

Following the reviewer suggestion we have tried to clarify the references to the Figures where it seemed confusing. Concerning Fig. 6, 8, and 10 they can be reproduced with a larger size in the published version of the paper. This will considerably help their clarity and quality.

The same profile (V28b) is shown in Fig. 6 (between 0 and 4000 m) and Fig. 10 (between 0 and 1500 m). V28 has been corrected in V28b in Fig. 10.

Specific comments:

Page 8292, section 3.2.: There is a bit of confusion about OPC and PCASP measurements. If another OPC (GRIMM) is onboard, avoid OPC for the PCASP.

The term “OPC” has been removed from the text and replaced with PCASP.

Page 8293, STP Conversion: line 7 and 8, ozone is measured using UV absorption. This technique is pressure dependent and pressure has to be taken into account. Does the MOZART instrument correct for pressure over all the altitude ranges?

The MOZART instrument itself does not correct pressure but it is connected to a pressurized inlet on-board the aircraft which compensates outside pressure drop during the flight. The pressure inside the inlet is maintained constant (and monitored) at 1020 hPa during the whole flight.

Page 8296, line 4-6, The text claims northeasterly winds, the data in Fig. 8 show northwesterly winds in altitudes above 1500 m.

The reviewer is correct and we stated north/north-easterly in spite of north/north-westerly, as shown both in Fig. 3 and 8. This error has been corrected in the text and in Table 1.

Page 8298, line 10: typical of pollution/anthropogenic particles. . . needs more description what is the ‘typical spectral variability

The sentence has been rewritten as: “For the different vertical soundings the particle concentrations dN_{Acc} and dN_{Coarse} vary in the range $\sim 100\text{-}3000\text{ cm}^{-3}$ and $\sim 5\text{-}4000\text{ cm}^{-3}$, respectively, for plumes with σ_s between 10 and 120 Mm^{-1} . The profile of the aerosol scattering coefficient is mostly correlated to dN_{Acc} , and this also reflects the pronounced spectral variability (i.e., decrease for increasing wavelength) of the scattering coefficient, typical of pollution/anthropogenic particles. dN_{Coarse} also contributes to the scattering signal in some cases especially at high altitudes (see V16, V20, V21, V22, and V23 above ~ 2000 m), and this reflects the low spectral variability of the scattering coefficient”.

Page 8299, lines 18 and 19: The manuscript states that these values are comparable with values measured close to the surface at urban continental sites but the references are taken from rural (Petzold), airborne (Mallet 2005), the proper reference is Mallet 2003, rural to suburban (Wiegner instead of Weigner) rural Po-Valley (Junkermann) airborne, (Hamburger).

Following the reviewer suggestion we have rewritten as: “The dN_{Acc} and dN_{Aitken} measurements within the BL and in the FT over the sea are comparable with the values measured close to the surface at continental sites under pollution conditions (Petzold et al., 2002; Mallet et al., 2003 and 2005; Wiegner et al., 2006; Junkermann, 2009; Hamburger et al., 2012).” Concerning the reference of Mallet et al., the papers of 2003 and 2005 analyses data acquired during the same campaign (ESCOMPTE in 2001) over the area of Marseille/Fos Berre. I have however added the Mallet et al. 2003 reference to the list.

I have also added the following reference to the comparison:

Highwood, E. J., Northway, M. J., McMeeking, G. R., Morgan, W. T., Liu, D., Osborne, S., Bower, K., Coe, H., Ryder, C., and Williams, P.: Aerosol scattering and absorption during the EUCAARI-LONGREX flights of the Facility for Airborne Atmospheric Measurements (FAAM) BAe-146: can measurements and models agree?, Atmos. Chem. Phys., 12, 7251-7267, doi:10.5194/acp-12-7251-2012, 2012.

Page 8300, section trace gas vertical profiles: The authors discuss ozone in freshly polluted and aged air masses. In freshly polluted air masses ozone is normally titrated with coemitted nitrogen oxide. In this case a peak in pollution (without other parameters probably here CO) would be visible together with a reduction of ozone in the same layer, see Figure 10. However, in the vertical profiles these features are not coincident. The particle peak is lower in altitude than the ozone dip. That's looking like a mismatch of the timing in the data. Very similar in V20 the clean layer in the scattering data are between 1600 and 200 m. the concurrent ozone peak is about 100 m lower. Such a timing mismatch can have consequences for the ozone / CO ratio which is used for further analysis.

We have verified and there are not mismatches between ozone and the other data shown in Fig. 8 and 10. In the different profiles O_3 appears mostly correlated with dN_{Acc} and vertical localization of the peaks is mostly coincident. However it should be taken in mind that the processes controlling particle concentration/optical properties and the gas chemistry may be not the same, and this can influence their vertical distribution.

Concerning the expected minimum in ozone in correspondence of fresh pollution plumes, it has to be pointed out that measurements are performed over the sea and not close to continental/urban sources, so it might be expected that the O_3 concentration within plumes can vary depending on the photochemical processes and on possible mixing occurring along pollution export over the sea, as well as the concentration of NO_x and VOC (Volatile Organic Compounds) at emission and their time evolution.

The estimation of the titration, in any case has not been possible during TRAQA when NO_x were not measured. During SAFMED, NO_x were measured and we observed titration of O_3 only in one case very locally above the sea surface (at about 150 m) in the gulf of Genoa during flight 51 (data in correspondence of a straight levelled run, not shown in this paper). This was possibly linked to fresh ship emissions. No other cases of O_3 titration were observed during SAFMED.

Page 8302, section 5.3. For the O_3 and CO ratios ‘typical’ values are given. This is not the case for the Aitken to accumulation number ratio. It would be good to have some idea about such ‘typical’ values.

We did not find in the literature some reference values for the Aitken to Accumulation particle mode ratio for pollution particles. We have found several references, but mostly for forest fires aerosols. If the reviewer has some references to suggest we would add it in the paper.

Page 8303, Section 5.3.1, Profile V19: Contrary to the text the profile shows values of about 3000 Aitken particles up to about 1500 m. the lowest values were measured just above, not below 800 m. This is just above the MBL as indicated and shows a peak in the accumulation mode and in the humidity. The ratio of Aitken to accumulation mode particles rises rapidly above 2500 m. This is not discussed in this section at all. It's mentioned a bit later in the text, but should be included here. Again there is an altitude mismatch between observations of increased Aitken mode particles that are described as fresh emissions and the concurrent ozone measurements.

The distinction of the two layers (the one below 800 m and the second one at 800-2600 m) has been performed based on the $dN_{\text{Aitken}}/dN_{\text{Acc}}$ and $\Delta O_3/\Delta CO$ profiles, which show a distinct behaviour at the two considered altitude ranges. The single profile of dN_{Aitken} does not permit to distinguish these two structures. We changed the text accordingly to clarify this point in the text. Additionally, we also mention here the presence of the layer above 2600 m characterized by high dN_{Aitken} .

Concerning the possible altitude mismatch between dN_{Aitken} and O_3 , see the answer to one of the previous comments.

Page 8304, Section 5.3.2 V20 The CO rich layer is only within the lowest 150 m. no data are presented in Fig. 8. Data in the figure are not always in agreement with the text. Lowest Aitken number concentrations at 380 m are very low, clearly below 1000 in the same altitude also the scattering coefficients are typical for the free troposphere.

The text has been changed as: "The aerosol profile in the BL is characterized in the first ~400 m by the presence of a layer richer in dN_{Aitken} ($dN_{\text{Aitken}}/dN_{\text{Acc}} > 20$) and CO (100 ppbv close to the surface; CO data not available between 150 and 650 m) possibly linked to fresh pollution, followed by the alternation of several layers characterized by a variable dN_{Aitken} (1000-6000 scm^{-3}) and lower CO (~70 ppbv). A local minimum of dN_{Aitken} and σ_s is found at ~400 m."

Page 8306, Line 22 ff. The initial text of the paragraph is confusing, first of all case studies are mentioned in Fig. 10, than several profiles are listed, but finally only two of those are included in the figures.

I guess the reviewer refers to page 8005. The initial text of the paragraph has been rewritten as: "For about half of the observed events the dN_{Aitken} layer presents a good correlation with dN_{Acc} , CO, and O_3 which suggests that the layer has been transported from a region directly emitting in this size range. These cases are: V16 at ~200-400 m, V21 at ~400-800 m, V28 at ~250 m, and V31 at ~1000-3000 m (only V28 and V31 are shown in Fig. 10).".

Pages 8305/8306, High Aitken number concentrations are described as originating from Valencia. That would require a very intense vertical mixing up to 3000 m. What is the reason for the low values in the marine Boundary layer, despite rather high values of CO (Fig. 10)?

The back-trajectories analysis indicates that in the boundary layer the air-masses have a different origin compared to the free troposphere. In particular, they come from the open sea (eastern of

Valencia) in the boundary layer. This can explain the different behaviour observed in the V31 profile. This point is specified in the text.

For reference, several papers have focussed on the export mechanisms in the Western Mediterranean basin within the lower troposphere, such as:

Millán, M. M., B. Artúñano, L. Alonso, M. Navazo, and M. Castro: The effect of meso-scale flows on the regional and long-range atmospheric transport in the western Mediterranean area, *Atmos. Environ.*, 25A, 949–963, 1991.

Velchev, K., Cavalli, F., Hjorth, J., Marmer, E., Vignati, E., Dentener, F., and Raes, F.: Ozone over the Western Mediterranean Sea – results from two years of shipborne measurements, *Atmos. Chem. Phys.*, 11, 675-688, doi:10.5194/acp-11-675-2011, 2011.

1 **Continental pollution in the Western Mediterranean basin: vertical profiles of**
2 **aerosol and trace gases measured over the sea during TRAQA 2012 and**
3 **SAFMED 2013**

4 C. Di Biagio¹, L. Doppler^{2,3,4}, C. Gaimoz¹, N. Grand¹, G. Ancellet², J.-C. Raut², M. Beekmann¹, A.
5 Borbon¹, K. Sartelet⁵, J.-L. Attié^{6,7}, F. Ravetta², and P. Formenti¹

6 (*corresponding author: claudia.dibiagio@lisa.u-pec.fr)

7
8 ¹ *LISA, UMR CNRS 7583, Université Paris Est Créteil et Université Paris Diderot, Institut Pierre*

9 *Simon Laplace, Créteil, France*

10 ² *Sorbonne Universités, UPMC Univ. Paris 06; Université Versailles St-Quentin; CNRS/INSU,*

11 *LATMOS-IPSL, Paris, France*

12 ³ *Freie Universität Berlin, Berlin, Germany*

13 ⁴ *Deutscher Wetterdienst, Meteorological Observatory Lindenberg, Germany*

14 ⁵ *CEREA, Joint Laboratory École des Ponts ParisTech – EDF R & D, Université Paris-Est, 77455*

15 *Marne la Vallée, France*

16 ⁶ *Laboratoire d'Aérodologie, University of Toulouse, UMR 5560 CNRS, France*

17 ⁷ *CNRM GAME UMR 3589 CNRS, METEO-FRANCE*

18
19 **Abstract**

20 In this study we present airborne observations of aerosol and trace gases obtained over the sea in the
21 Western Mediterranean basin during the TRAQA (TRansport and Air QuAlity) and SAFMED
22 (Secondary Aerosol Formation in the MEDiterranean) campaigns in summers 2012 and 2013. A
23 total of 23 vertical profiles were measured up to 5000 m above sea level over an extended area

24 (40°-45°N latitude and 2°W-12°E longitude) including the Gulf of Genoa, Southern France, the
25 Gulf of Lion, and the Spanish coast. During TRAQA and SAFMED the study area
26 experienced~~successfully measured a w a~~ wide range of meteorological conditions ~~which~~which
27 favoured the pollution export from different sources located around the basin. Also, several events
28 of dust outflows were measured during the campaigns. Observations from the present study
29 indicatesshow that continental pollution largely affects the Western Mediterranean both close to
30 coastal regions and in the open sea as far as ~250 km from the coastline. ~~Aerosol layers not~~
31 ~~specifically linked with Saharan dust outflows are distributed ubiquitously which indicates quite~~
32 ~~elevated levels of background pollution throughout the Western basin.~~ The measured aerosol
33 scattering coefficient varies between ~20 and 120 Mm⁻¹, while carbon monoxide (CO) and ozone
34 (O₃) mixing ratios are in the range of 60-~~170~~-165 ppbv and 30-85 ppbv, respectively. Pollution
35 reaches 3000-4000 m in altitude and presents a very complex and highly stratified structure
36 characterized by fresh and aged layers both in the boundary layer and in the free troposphere.
37 Within pollution plumes the measured particle concentration in the Aitken (0.004-0.1 μm) and
38 accumulation (0.1-1.0 μm) modes is between ~100 and 5000-6000 scm⁻³ (standard cm⁻³), which is
39 comparable to the aerosol concentration measured in continental areas under pollution
40 condition~~continental urban areas~~. Additionally, our measurements indicate the presence of highly
41 concentrated Aitken layers (10000-15000 scm⁻³) observed both close to the surface and in the free
42 troposphere, possibly linked to the influence of new particle formation (NPF) episodes over the
43 basin.

44

45 1. Introduction

46 Atmospheric aerosols play an important role on climate through their participation to several
47 chemical, dynamical, and radiative processes. At present, still large uncertainties persist in the

48 estimation of the aerosol direct and indirect effects mainly due to the difficulty of fully
49 characterizing their spatial and vertical distribution and properties (Boucher et al., 2013).

50 The Mediterranean region is a complex area where atmospheric aerosols of different origins and
51 types may be found (Pace et al., 2006; Kallos et al., 2007; Gkikas et al., 2012). High levels of
52 anthropogenic aerosol particles and pollutants are measured in the Mediterranean (Lelieveld et al.,
53 2002), which is also indicated as one of the main hot spots for air quality issues (Monks et al.,
54 2009).

55 The North-Western part of the Mediterranean basin, due to its proximity to highly polluted
56 industrialized areas (such as the Po Valley in northern Italy and the Fos/Berre in southern France)
57 and large coastal cities (Barcelona, Genoa, Marseilles, Nice, or Valencia), is frequently affected by
58 continental outflows and severe pollution episodes (Mallet et al., 2005; Pérez et al., 2008; Pey et al.,
59 2010). The strength of these episodes is particularly intense during summer when stable
60 meteorological conditions and the high level of insolation promote photochemical reactions and the
61 build-up of ozone and other pollutants (e.g. Millán et al., 2000).

62 A number of studies have investigated the dynamics of pollution export over the Western basin with
63 the aim of characterizing the impact of anthropogenic emissions over this region. Most of these
64 studies have been conducted in continental coastal areas and provide information on the vertical
65 distribution of aerosols and their properties mainly close to local pollution sources. They include
66 ground-based observations with lidars (Soriano et al., 2001; Pérez et al., 2004; Ancellet and
67 Ravetta, 2005), and airborne campaigns, such as MECAPIP (MEso-meteorological Cycles of Air
68 Pollution in the Iberian Peninsula) and RACAPMA (RegionAl Cycles of Air Pollution in the west
69 central Mediterranean Area) in coastal Spain (Millán et al., 1996 and 1997) and ESCOMPTE
70 (Experience sur Site pour Contraindre les Modeles de Pollution atmospherique et de Transport
71 d'Emissions) in Southern France (Drobinski et al., 2007). The results of these studies have
72 highlighted the important role of pollution in modulating the atmospheric composition in this part

73 of the basin, as well as the high variability of the aerosol distribution and properties in link to
74 different export conditions (Flamant and Pelon, 1996; Soriano et al., 2001; Mallet et al., 2005). In
75 particular, the interaction between synoptic circulation and local dynamics, such as orography and
76 sea breezes, has been shown to strongly impact the vertical distribution, layering, and aging of
77 particles along coastal regions (e.g. Millan et al., 1997; Gangoiti et al., 2001; Pérez et al., 2004;
78 Velchev et al., 2011).

79 The capability of reproducing this complexity by air quality models represents a real challenge
80 (Jimenez et al., 2006; Jiménez-Guerrero et al., 2008), and experimental observations gives a
81 fundamental support to test the performances of the model outputs over the Western Mediterranean
82 environment.

83 The large set of observations conducted in the last decades has permitted to acquire a detailed
84 characterisation of pollution aerosols in the surroundings of the Western basin. However, at the
85 present time we miss an extensive representation of the mean aerosol load, distribution, and
86 properties in the whole region, in particular over the remote sea. In addition, there is a significant
87 lack of observations over some key areas, as for example the Gulf of Genoa, directly under the
88 influence of the outflow from the highly polluted Po Valley (Velchev et al., 2011).

89 In this study we present measurements of aerosols and trace gas vertical profiles acquired during 24
90 scientific flights performed with the ATR-42 French research aircraft during the TRAQA
91 (TRansport and Air QuAlity) and SAFMED (Secondary Aerosol Formation in the MEDiterranean)
92 campaigns in summers 2012 and 2013 in the framework of the Chemistry-Aerosol Mediterranean
93 Experiment (CHARMEX, <https://charmex.lsce.ipsl.fr/>). The TRAQA and SAFMED flights
94 explored an extended region of the Western Mediterranean basin between 40°-45°N latitude and
95 2°W-12°E longitude including the Gulf of Genoa, Southern France, the Gulf of Lion, and the
96 Spanish coasts. Measurements were performed over the sea at various distances from the coastline
97 with lidar and in situ instruments. During TRAQA and SAFMED the Western basin was **interested**

98 | ~~by~~under diverse synoptic conditions which led to the occurrence of different pollution export
99 regimes (Mistral/Tramontane events, outflow from the Po Valley and the Iberian Peninsula) and
100 allowed sampling atmospheric aerosols of different origin and types.

101 | The main objective of the present work is to provide ~~extensive~~ observations of the vertical
102 distribution of aerosols and trace gases related to the export of anthropogenic pollution at the
103 regional scale of the Western Mediterranean basin. The detailed knowledge of the vertical structure
104 of the atmosphere is very important to understand the impact of continental pollution over the basin.
105 The paper is organized as follows: in Sections 2, 3, and 4 we describe the flight trajectories and
106 strategy during TRAQA and SAFMED, the in situ measurements carried out on board the ATR-42
107 aircraft, and the meteorological conditions observed during the campaigns. In Sect. 5 we present the
108 results. The aerosols and trace gases vertical profiles are shown in Sections 5.1 and 5.2. Section 5.3
109 is dedicated to analyse the variability of the pollution plume composition and atmospheric structure
110 also in link with the different outflow conditions. Airborne measurements in presence of layers with
111 high concentrations of fine particles are discussed in Section 5.4. The main conclusions are reported
112 in Section 6.

113

114 **2. Overview over flights**

115 Figure 1 shows the trajectories of the flights performed during the TRAQA (20 June-13 July 2012)
116 and the SAFMED (24 July-1 August 2013) campaigns. Research flights were performed with the
117 SAFIRE (Service des Avions Français Instruments pour la Recherche en Environnement,
118 <http://www.safire.fr/>) tropospheric aircraft ATR-42. The aircraft has a maximum endurance of 4 h.
119 The flight altitude ranges between a minimum of ~60 m over the sea, to a maximum of ~5000 m
120 above sea level (a.s.l.). The aircraft was based in Toulouse (43°36'N, 1°26'E, France) during
121 TRAQA and in Genoa (44°24'N, 8°55'E, Italy) during SAFMED. Twenty-four flights for a total of
122 ~75 hours of data have been collected. Seventeen of the twenty-four flights presented in the paper

123 were performed during TRAQA (flight numbers V16 to V32) and 7 during SAFMED (V46 to
124 V52). All flights were carried out during daytime, when light-induced chemistry favours the
125 pollution levels. Frequently, two flights per day, with intermediate stops in different airports in
126 Southern France, Corsica, and Sardinia, were performed. The majority of flights were over the sea,
127 with some exceptions investigating inland areas in Southern France and central Italy. Main
128 information concerning the TRAQA and SAFMED flights is summarized in Table 1.

129 The general flight strategy consisted in plane flights with lidar observations and vertical
130 ascents/descents to sound the vertical atmospheric column (from ~60-100 m to 3000-5000 m a.s.l.)
131 and identify main meteorological and aerosol features, followed by straight levelled runs (SLRs)
132 within the detected aerosol layers. In this study we focus on vertical profiles data. A total of 23
133 profiles were acquired in 20-30 minutes each by performing a spiral trajectory ~10-20 km wide.
134 Fig. 1 also identifies the geographical position of each sounding. As shown in Fig. 1 the profiles
135 were performed at different distances from the coastline, from a minimum of ~5-10 km for V31 and
136 V32 to more than ~250 km for V20 and V25, and covered almost all the different sectors of the
137 Western basin.

138

139 **3. Measurements and methods**

140 The basic equipment of the ATR-42 aircraft includes sensors for the measurements of
141 meteorological parameters (pressure, temperature, relative humidity, wind components), radiative
142 fluxes (down- and up-welling shortwave and longwave radiation), and carbon monoxide (CO) and
143 ozone (O₃) mixing ratios.

144 Aerosol sampling was performed using the AVIRAD system (Formenti et al., 2011). AVIRAD is an
145 iso-axial and iso-kinetic inlet which, at the normal cruise speed of the ATR-42 (~93 m s⁻¹), samples
146 air at a volumetric flow of ~350 l min⁻¹. The 50% passing efficiency of the inlet was tested to be 12
147 μm diameter. Various sampling lines depart from AVIRAD to connect to different instruments

148 mounted inside the aircraft cabin: (i) a 3-wavelength nephelometer (TSI Inc., model 3563) for the
149 measurement of the dry particle volume total scattering (σ_s) and hemispherical backscattering (σ_{bs})
150 coefficients at 450, 550, and 700 nm; (ii) a 7-wavelengths aethalometer (Magee Sci., model AE31)
151 for the measurement of the particle absorption coefficient (σ_a) at 370, 470, 520, 590, 660, 880, and
152 950 nm; (iii) an optical particle counter (~~OPC~~) (GRIMM Inc., model 1.129) for the measurement of
153 the particle number concentration over 32 size classes between 0.3 and 32 μm in diameter; (iv) a
154 Condensation Particle Counter (CPC, TSI Inc., model 3775) for the measurement of the total
155 particle number concentration in the diameter range 0.004-3.0 μm ; and (v) 3 lines for aerosol
156 sampling on filter membranes and a 4-stage cascade impactor (Dekati Inc) to measure the bulk and
157 size-segregated particle composition. In addition, the ATR-42 was equipped with a Passive Cavity
158 Aerosol Spectrometer Probe (PCASP, model 100X) ~~OPC~~ optical particle counter for the
159 measurement of the aerosol number concentration over 31 size classes between 0.1–3.0 μm . The
160 PCASP was installed outside the cabin on the left side of the aircraft fuselage.

161 In this study we consider measurements of the (i) aerosol scattering coefficient from the
162 nephelometer, (ii) particle concentration from the CPC and PCASP instruments (GRIMM data are
163 not considered since they are available only below ~350 m during TRAQA), (iii) CO and O₃ trace
164 gases from the MOZART analyser, and (iv) meteorological parameters from the ATR-42 sensors. A
165 more detailed description of the nephelometer, CPC, PCASP, and MOZART measurements and
166 their data analysis is provided in the following sections.

167 The present analysis is based only on measurements obtained in cloud free conditions.

168

169 **3.1 Aerosol scattering coefficient**

170 A three-wavelength integrating nephelometer has been used to measure the dry particle volume
171 total scattering (σ_s) coefficient at 450, 550, and 700 nm. The sampling flow rate was 30 l min⁻¹.
172 Data were acquired at 6 s resolution during TRAQA and 1 s resolution during SAFMED. The

173 instrument was calibrated prior ~~the~~each campaign with free-particle air and CO₂ as gases of low
174 and high known scattering coefficient. Nephelometer measurements have been corrected for angular
175 truncation and Lambertian non-idealities by applying the formulae by Anderson and Ogren (1998).
176 The measurement uncertainty on σ_s is calculated taking into account for the photon counting, gas
177 calibration, and angular corrections uncertainties (Anderson et al., 1996; Anderson and Ogren,
178 1998). The total uncertainty on σ_s is estimated to be lower than 10% at the three wavelengths.

179 The nephelometer measured the scattering coefficient in dry air conditions. This is due to the
180 heating of the airflow while entering the aircraft cabin and the temperature in the cavity of the
181 instrument. The relative humidity measured during the flights inside the nephelometer was <25% in
182 more than ninety percent of cases, with values up to ~40% occasionally observed at very low
183 altitudes (<200 m) over the sea surface. A possible underestimation of the scattering coefficient
184 may thus occur in case of hygroscopic aerosols, especially under high relative humidity conditions
185 in the atmosphere.

186 The particle scattering Ångström exponent (α_s) has been calculated from spectral nephelometer
187 measurements with a power-law fit of the measured scattering coefficients versus wavelength.

188

189 **3.2 Aerosol particle number concentration**

190 The vertical profiles of the total particle number concentration in the Aitken (dN_{Aitken} , 0.004-~~nm~~0.1
191 μm), accumulation (dN_{Acc} , 0.1-1.0 μm) and coarse (dN_{Coarse} , >1.0 μm) modes have been obtained
192 by combining CPC and PCASP data. The CPC and the PCASP measured at a sample flow of 1.5
193 and 0.06 l min⁻¹, respectively, and with a time resolution of 1 s for the PCASP and 5 s and 1 s for
194 the CPC during TRAQA and SAFMED, respectively.

195 The PCASP was factory calibrated with monodisperse polystyrene sphere latex (PSL) whose
196 complex refractive index at the instrument operating wavelengths (632.8 nm) is 1.59-0i. The

197 measured sphere-equivalent optical diameter has been converted to a sphere-equivalent geometrical
198 diameter (D_g) by taking into account the complex refractive index of the sampled aerosol (Liu and
199 Daum, 2000). Given that in the very large majority of cases the aerosol sampling during TRAQA
200 and SAFMED was associated to the export of pollution plumes, only pollution aerosols have been
201 considered for ~~OPC~~PCASP correction. Note that these data are not optimized for dust or marine
202 aerosol observations. A large interval of values ($n \sim 1.50-1.72$, $k \sim 0.001-0.1$ for UV-visible
203 wavelengths) are reported in the literature for the real and the imaginary parts of the refractive index
204 for anthropogenic aerosols over Europe (e.g., Ebert et al., 2002 and 2004; Müller et al., 2002;
205 Mallet et al., 2003 and 2011; Chazette et al., 2005; Raut and Chazette, 2008). For our calculations at
206 632.8 nm we have fixed the imaginary part of the refractive index to 0.01, thus representing a mean
207 absorbing aerosol, and then we have varied the real part between its minimum (1.50) and maximum
208 (1.72) reported value. D_g is then set at the mean \pm one standard deviation of the values obtained for
209 the different values of n . We assume in these calculations that the refractive index does not vary
210 with height. After refractive index correction the D_g range for the PCASP becomes 0.10-4.47 μm ,
211 with an uncertainty between 1 and 25%. The smallest and the largest size bins of the ~~OPC~~PCASP,
212 for which the minimum and maximum edges respectively are not defined, have been excluded from
213 the datasets, thus reducing the PCASP D_g range to 0.11-4.17 μm .

214 Once corrected for the refractive index, PCASP data have been combined with those from the CPC
215 to calculate dN_{Aitken} , dN_{Acc} , and dN_{Coarse} . Values for dN_{Acc} and dN_{Coarse} are obtained by integrating
216 the PCASP number concentrations in the 0.1-1.0 μm and 1.0-4.17 μm ranges, while dN_{Aitken} is
217 estimated as the difference between CPC concentration and the integral of PCASP data between 0.1
218 and 3.0 μm . The comparison between the PCASP and the GRIMM below 350 m altitude indicates
219 that the former underestimates by about 50% the aerosol concentration in the range 0.4-1.0 μm (the
220 accuracy of the GRIMM has been verified by optical closure study against simultaneous aircraft
221 nephelometer measurements). This is estimated to induce a $\sim 20\%$ underestimation of the dN_{Acc}

222 calculated here. Conversely, the PCASP underestimation in the 0.4-1.0 μm range has almost a
223 negligible impact on $\text{dN}_{\text{Aitken}}$.

224 CPC measurements, and so $\text{dN}_{\text{Aitken}}$ data, were not available during SAFMED flights V49, V50, and
225 part of V51.

226

227 **3.3 Trace gases**

228 Carbon monoxide (CO) and ozone (O_3) mixing ratios were measured by the MOZART instrument
229 described in detail by Nedélec et al. (2003). CO is a long-lived tracer for air masses influenced by
230 combustion processes, whereas O_3 in the troposphere is a photochemical product of the oxidation of
231 CO and volatile organic compounds (VOCs) in the presence of nitrogen oxides (NO_x). CO and O_3
232 are measured at a resolution of 30 s and 4 s, respectively. The nominal uncertainty is $\pm 5\%$ for CO
233 and $\pm 2\%$ for O_3 (Nedélec et al., 2003). However, a recent airborne intercomparison in May 2014 in
234 the framework of the French ChemCalInt project and the TGOE European Joint Research Activity
235 has suggested a greater uncertainty (up to 30%) on CO measurement by MOZART on-board the
236 ATR-42 (A. Borbon, personal communication, 2015). Trace gas analysis will focus mostly on the
237 vertical distribution of the $\Delta\text{O}_3/\Delta\text{CO}$ ratio rather than absolute concentrations (see section 5.3) and
238 the uncertainty on CO should not affect data interpretation.

239

240 **3.4 STP conversion**

241 In order to compare measurements obtained at different altitudes the data presented here are
242 reported at standard temperature and pressure (STP) using $T=293.15$ K and $p=1013.25$ hPa (NIST,
243 National Institute of Standards and Technology, values). Hence, the scattering coefficient is scaled
244 to STP conditions and the particle concentrations are given as particles per standard cm^{-3} (scm^{-3}).

245 For a generic parameter x measured at the temperature T and pressure p , the conversion at STP is
246 ~~done-calculated~~ with the formula:

$$247 \quad x(\text{STP}) = x(T, p) \frac{T}{293.15} \frac{1013.25}{p} \quad (1).$$

248 CO and O₃ do not need to be corrected for STP since the mixing ratio does not depend on
249 temperature and pressure.

250

251 3.5 Meteorological parameters

252 The vertical profiles of the pressure (p), the temperature (T), the relative humidity (RH) and the
253 wind components towards the east and the north (U , V) measured on board the ATR-42 have been
254 used to analyse the atmospheric structure during flights. Starting from the measured parameters the
255 potential temperature (θ) has been also calculated as $\theta = T(p_0/p)^{0.286}$ with $p_0=1013.2$ mbar. For
256 each profile the height of the marine aerosol boundary layer (MABL) and planetary boundary layer
257 (BL) has been estimated visually by looking at the vertical gradients of T , θ , and RH.
258 Meteorological parameters have been also used to calculate the vertical profiles of the gradient
259 Richardson number (Ri):

$$260 \quad \text{Ri} = \frac{g}{\theta} \frac{\partial \theta}{\partial z} \bigg/ \left(\left(\frac{\partial U}{\partial z} \right)^2 + \left(\frac{\partial V}{\partial z} \right)^2 \right) \quad (2).$$

261 In Eq. (2) g is the gravitational acceleration and z is the height. The Ri number is the ratio between
262 the buoyancy force and the wind shear and it is used to indicate dynamic stability and the formation
263 of clear air turbulence. Turbulence can develop when Ri is below the critical threshold $\text{Ri}_{\text{crit}}=0.25$,
264 while it is inhibited for $\text{Ri}>1$ (e.g., Wallace and Hobbs, 2006). In this study the profiles of Ri are

265 used to provide indications of favorable/unfavorable conditions for the development of turbulent
266 conditions within the atmosphere.

267

268 **3.6 Tracking the air mass back-trajectories**

269 The Lagrangian trajectory model FLEXTRA (FLEXible TRAjectories, Stohl et al., 1995) has been
270 used in selected cases to track the origin of sampled air masses. Five days three-dimensional back-
271 trajectories have been calculated using the ECMWF (European Centre for Medium-Range Weather
272 Forecast) operational analysis with a 0.5° by 0.5° horizontal resolution and up to 30 vertical model
273 levels below 4000 m. The model specific humidity and potential vorticity is also interpolated along
274 the trajectory path.

275

276 **4. Meteorological conditions, aerosol load, and pollution export regimes**

277 In order to characterize the general aerosol conditions encountered over the Western Mediterranean
278 basin during the TRAQA and the SAFMED campaigns we have plotted the time-series of the
279 aerosol optical depth ($\tau_{\pm 0.02}$) at 440 nm and the 440-870 nm Ångström exponent (α) measured
280 with a Cimel sunphotometer (Holben et al., 1998) at the three AERONET stations of Barcelona,
281 Frioul, and Erso located along the coast around the Western basin (see Fig. 1). Level 1.5 cloud-
282 screened data are used in this study. Data are shown in Fig. 2 and correspond to the period of the
283 campaign of measurements plus 10 days before and after. Table 1 reports the date, location, and
284 main meteorological and export conditions encountered during TRAQA and SAFMED flights.

285

286 ~~The TRAQA campaign in 2012 was characterized by very variable meteorological conditions which~~
287 ~~prevented the accumulation of high levels of pollutants over the basin. Over the analysed~~
288 AERONET sites ~~t~~The aerosol optical depth was below 0.2 before the beginning of the TRAQA

289 campaign ~~over the whole basin~~ and increased, especially at Barcelona and Ersar, to ~0.3-0.5 (with
290 $1 < \alpha < 2$) in the periods 23-26 June and 3-13 July 2012. Isolated peaks of τ were measured in
291 correspondence of two Saharan dust intrusion events which occurred on the 17-23 June ($\tau \sim 0.6$) and
292 29 June 2012 ($\tau \sim 1.4$). Different wind regimes occurred during TRAQA and favoured the
293 continental outflow from different regions located around the basin. Two examples of wind maps
294 derived from WRF-Chem model (Grell et al., 2005) at 925 mbar are shown in Fig. 3 for 26 June and
295 3 July 2012. Main observed meteorological/export conditions can be summarized as follows: (i) on
296 26-27 June north/north-weasterly winds blew across northern Italy determining an air mass outflow
297 towards the Gulf of Genoa (measurements on flights V18-V19-V21); (ii) on the same days a strong
298 Mistral-Tramontane episode (i.e., strong northerly winds developing along the Rhône and Aude
299 valley which bring a northerly/north-westerly flow over the Western Mediterranean, see Fig 3a)
300 favoured the dispersion of pollutants towards the central part of the Western basin. Measurements
301 during the event were performed during flight V20; (iii) on 3-4 July the wind regime was dominated
302 by westerly/south-westerly winds mostly blowing at the surface across the Iberian Peninsula and
303 southwestern France (see Fig. 3b). This condition allowed measuring the export of pollution from
304 the Spanish coasts, in particular close to the area of Barcelona (flights V24-V25-V26, see Fig. 31).
305 Additionally, flight V31 sounded the atmospheric structure close to the Spanish coasts -reaching the
306 southern urban area of Valencia. The flight was performed under the influence of south-westerly
307 winds favouring the export from the Iberian Peninsula towards the basin; (iv) ~~moderate~~-Mistral
308 episodes occurred on the 6-7 and 11 July 2012. In those cases the Mistral wind combined with a
309 persistent westerly flow thus yielding pollution export towards the central and central-eastern part
310 of the Western basin, as measured during flights V27-V28-V30-V32; (v) finally, Saharan dust
311 aerosols were sampled during flights V16 and V20 (episode of the 17-23 June) and flights V22 and
312 V23 (episode of the 29 June).

313 During SAFMED the meteorological conditions were more stable and two distinct phases were
314 observed: (i) a stable anticyclone affected the whole Western Mediterranean area during the first
315 half of July until the 26th, thus possibly favouring a more pronounced accumulation of
316 photochemical pollution in this part of the basin. Relatively high values of both τ (~0.2-0.8) and α
317 (~1-2.5) were measured at the three sites of Barcelona, Frioul, and Ersa in this period; (ii) a
318 cyclonic system moving from the Atlantic region towards Europe then affected the Western basin
319 on 28-29 July 2013. Very clean conditions ($\tau < 0.1-0.2$) were measured afterwards over the entire
320 region until the end of the SAFMED campaign. Winds were mostly westerly/south-westerly in the
321 first period of the campaign (24-29 July 2013, flights V46, V47, V48, V49, V50), which means that
322 the sampled air flow came mostly from the sea. Then, from 30 July to 1 August 2013 a north-
323 easterly flow affected the SAFMED investigated area thus promoting the export of pollution from
324 Northern Italy towards the Gulf of Genoa (flights V51, V52). A strong Mistral event (29 July-1
325 August) and two Saharan dust outbreaks (27-28 July and 1 August) affected the Western basin,
326 however not influencing the vertical profile observations during SAFMED.

327 In order to identify the distribution of observations during TRAQA and SAFMED as a function of
328 the aerosol type we have plotted in Figure 4 the distribution of the measured scattering coefficient
329 σ_s at 450, 550, and 700 nm as a function of the calculated scattering Ångström exponent α_s for all
330 vertical profiles. The plot shows a similar scattering intensity between cases dominated by coarse
331 particles ($\alpha_s < 0.5-1.0$), such as desert dust, and those dominated by fine particles ($\alpha_s > 1.0-1.5$), such
332 as pollution aerosols. For both dust and pollution σ_s peaks at about 100-120 Mm^{-1} . The frequency of
333 occurrence of α_s shows that pollution plumes represent the large majority of the cases observed,
334 with more than 70% of measurements with $\alpha_s > 1.0$.

335

336 5. Results

337 Figure 5 shows the box and whisker plots of the aerosol scattering coefficient σ_s at 450, 550, and
338 700 nm, particle number concentration in the Aitken (dN_{Aitken}) and accumulation (dN_{Acc}) and coarse
339 (dN_{Coarse})-diameter ranges, and CO and O₃ measured in the boundary layer (BL) and in the free
340 troposphere (FT) within pollution plumes for all the different vertical soundings analysed in this
341 study. This plot summarizes the range of values observed during TRAQA and SAFMED. On
342 average, the scattering coefficient and CO are larger in the BL compared to the FT, whilst similar
343 ranges of values are measured in the two regions for dN_{Aitken} , dN_{Acc} , and O₃. Even within the single
344 BL and FT the different parameters show a large variability that will be explored in the following
345 paragraphs.

346

347 **5.1 Vertical profiles of aerosol concentration and scattering coefficient**

348 Figure 6 shows the vertical profiles of σ_s , dN_{Acc} , and dN_{Coarse} during TRAQA and SAFMED flights.
349 The date, time and coordinates of each profile, as well as the heights of the top of the marine and
350 planetary boundary layer (MABL and BL) estimated from meteorological data are also indicated in
351 the plot.

352

353 For the different vertical soundings the particle concentrations dN_{Acc} and dN_{Coarse} vary in the range
354 ~~~1000-32000~~ ~3200-32000 scm^{-3} and ~~~5-4000~~ ~5-4000 scm^{-3} , respectively, for plumes with σ_s between 10 and 120
355 Mm^{-1} . The structure in the scattering profile is generally mirrored in dN_{Acc} . The profile of the
356 aerosol scattering coefficient is mostly correlated to dN_{Acc} , and this also reflects the pronounced
357 spectral variability (i.e., decrease for increasing wavelength) of the scattering coefficient, typical of
358 pollution/anthropogenic particles. dN_{Coarse} also contributes to the scattering signal in some cases
359 especially at high altitudes (see V16, V20, V21, V22, and V23 above ~2000 m), and this reflects the
360 low spectral variability of the scattering coefficient. These observations are associated to the dust
361 intrusion episodes which occurred in the Western Mediterranean basin during TRAQA, which

362 however will not be analysed in detail here. Aerosol layers affected by dust have been labelled with
363 a “D” in Fig. 6.

364 Maxima of the scattering coefficient have been measured for TRAQA flights V21 and V23 (~120
365 Mm^{-1} for pollution_ in the BL and ~100 Mm^{-1} in the dust layer), whereas flights V46-V48-V49,
366 during the first and more polluted phase of SAFMED, are the richest in dN_{Acc} (1500-3000 scm^{-3}
367 over the whole column). Minima of σ_s and dN_{Acc} are obtained for flight V51 at the beginning of the
368 second SAFMED phase when clean conditions were observed in the Western Mediterranean.

369 Pollution plumes observed in the different flights extend from the boundary layer to the free
370 troposphere up to 3000-4000 m altitude. The vertical structure of the aerosol scattering
371 coefficient/particle concentration is linked to the variability of the atmospheric thermodynamic
372 structure and is generally characterized by a first layer confined in the MABL (<400 m, profiles
373 V16, V20, V22, V25, V48, V51), followed by one or more layers within the BL. In the FT pollution
374 particles occur both as single isolated plumes each about 500-1000 m deep (V21, V24, V25, V30,
375 V46, V49), or as a more uniform layer extending from the top of the BL up to 2500-4000 m altitude
376 (V26, V27, V28, V32, V48). The highest values of both the scattering coefficient and dN_{Acc} for
377 pollution are found within the MABL or BL in most cases, while a local minimum of σ_s and dN_{Acc}
378 is generally identified at the top of the BL. The scattering coefficient and the particle concentration
379 measured in the FT are comparable with the values observed in the BL, and in few cases even larger
380 (V25, V26, V30). Only in one case (profile V31) σ_s and dN_{Acc} decrease monotonically with height.
381 The aerosol vertical distribution, both in the BL and in the FT, often presents a strongly stratified
382 structure characterized by the presence of several thin sub-layers within one main identified aerosol
383 plume, as it can be seen in particular in the dN_{Acc} profiles (V20, V21, V22, V25, V46, V49).

384 The particle concentration in the Aitken mode (0.004-0.1 μm ; $\text{dN}_{\text{Aitken}}$, not shown in Fig. 6) is
385 generally below 5000-6000 scm^{-3} at all altitudes up to 4000 m within pollution plumes. $\text{dN}_{\text{Aitken}}$ is
386 correlated with dN_{Acc} in most of the observed cases, which indicates the common source of particles

387 in these two size ranges. Few layers exceeding $\sim 10000\text{-}15000\text{ scm}^{-3}$ are observed occasionally both
388 in the BL and in the FT. These will be discussed in more detail in Sect. 5.4.

389 The dN_{Acc} and dN_{Aitken} measurements within the BL and in the FT over the sea are comparable with
390 the values measured close to the surface at ~~urban~~-continental sites under pollution conditions ([see](#)
391 [Table 2](#)) (Petzold et al., 2002; Mallet et al., [2003 and](#) 2005; Weiegner et al., 2006; Junkermann,
392 2009; Hamburger et al., 2012; [Highwood et al., 2012](#)). This suggests that the export towards the
393 basin favours the redistribution of the pollution plumes along the vertical. Because of mixing in the
394 BL, measured concentrations within the BL can be as high as those observed close to the surface
395 ~~over at urban~~-continental ~~als~~-site under pollution conditions. Values of dN as high as in the BL are
396 observed in the FT because of transport in specific conditions, as discussed below.

397 The observations of aerosol profiles obtained during TRAQA and SAFMED are representative of
398 the complex transport regimes which characterizes the export towards the Western basin and that is
399 mostly determined by the interaction between regional meteorology and local dynamics (e.g.,
400 Gangoiti et al., 2001). A first example is associated to the measurements in the area of Barcelona.
401 As discussed in Pérez et al. (2004) the presence of mountains up to $\sim 500\text{-}3000$ m altitude a few
402 kilometres inland favours, during summertime, the recirculation of pollutants along the coasts of
403 Spain. In these cases, the aerosols emitted at the surface in coastal areas are transported inland and
404 uplifted by sea breezes and mountain winds then the plumes are re-injected at different altitudes and
405 distances from the coast. During the TRAQA flights V24, V25, and V26, under the influence of
406 pollution outflow from the Barcelona area, we detected the presence of aerosol layers with elevated
407 concentrations ($dN_{\text{Acc}} \sim 2000\text{-}3000\text{ scm}^{-3}$) up to 3500 m altitude at a distance of ~ 30 to 250 km from
408 the coast of Spain. Another example of complex dynamics linked to coastal orography is that
409 associated to the export from northern Italy and the Po Valley towards the Gulf of Genoa. The
410 presence of the Apennine Mountains close to the Ligurian coasts (max elevation $\sim 1500\text{-}2000$ m)
411 causes the uplift of continental air masses so determining the injection of aerosol plumes at different

412 altitudes both inside and outside the BL. Examples are given by flights V19, V21 and V52 for
413 which pollution aerosols from northern Italy are measured up to ~2000-3000 m altitude throughout
414 the Gulf of Genoa. Finally, another meteorological condition which largely influences the aerosol
415 export and distribution over the Western Mediterranean is the Mistral/Tramontane wind regime.
416 Under the influence of the Mistral flow, atmospheric aerosols can be dispersed as far as hundreds of
417 kilometres over the open sea, as discussed by Salameh et al. (2007). Examples are given in profiles
418 V20 and V28, performed at more than 100 km from the French coasts, for which pollution layers
419 associated to a Mistral flow are measured up to 2000-3000 m altitude.

420

421 **5.2 Trace gases vertical profiles**

422 Figure 7 shows O₃ versus CO for all TRAQA and SAFMED flights, while examples of CO and O₃
423 profiles representatives of different conditions are reported in Fig. 8 and 10.

424 CO and O₃ vary in the range 60-1~~6570~~ ppbv and 30-85 ppbv, respectively. The 25th and 75th
425 percentiles are 87 and 105 ppbv for CO and 49 and 62 ppbv for O₃, representative of moderate
426 pollution conditions (i.e., Parrish et al., 1998). By comparison, the values measured over land in
427 central Italy during flight V49 are in the range 80-180 ppbv for carbone monoxide and 40-85 ppbv
428 for ozone. CO and O₃ are generally correlated (correlation coefficient $R^2 \sim 0.5-0.8$) within measured
429 pollution plumes, and also correlated with σ_s and N_{Acc} both in the BL and in the FT, which indicates
430 photochemically active plumes. CO is generally higher in the BL, and shows absolute maxima in
431 the lowest levels (V20, V21, V24, V28, V46), then it decreases in the FT. Ozone presents a more
432 complicated vertical structure due to the different photochemical and dynamical processes which
433 control its formation and distribution. At first, local peaks of O₃ correlated with CO are observed in
434 correspondence of pollution plumes both in the BL and in the FT. An absolute maximum of O₃ is
435 sometimes found near the top of the BL (V24, V25, V30) possibly due to aged air masses trapped in
436 the boundary layer. Isolated peaks of O₃ (~75-80 ppbv) not correlated with aerosols and CO are also

437 measured in few cases above 3000-3500 m (V21, V25, V27, V28, V52). The analysis of back-
438 trajectories indicates that these high-altitude ozone layers are associated to the descent of air masses
439 travelling at about 7-8 km, which thus may suggest a downward transport from the upper
440 troposphere or the tropopause region due to a stratosphere-troposphere exchange (Ancellet and
441 Ravetta, 2005). Finally, absolute minima of O₃ (~15-30 ppbv) are measured within the dust layers
442 during flights V20 and V21, maybe related to the dust/ozone heterogeneous reactions which leads
443 to O₃ destruction, as documented in several studies (Bonasoni et al., 2004; Haywood et al., 2011).

444

445 **5.3 $\Delta O_3/\Delta CO$ and dN_{Aitken}/dN_{Acc} ratios and variability of pollution plume composition**

446 Using the O₃, CO, dN_{Aitken} and dN_{Acc} measurements we have estimated:

- 447 - the O₃-CO enhancement ratio ($\Delta O_3/\Delta CO$), i.e. the ratio of the ozone to carbon monoxide
448 variations compared to their baseline values. The $\Delta O_3/\Delta CO$ enhancement ratio is frequently
449 used to estimate the efficiency of O₃ formation and its export (Parrish et al., 1993; Zhang et
450 al., 2006). From our observations (Fig. 7) we have estimated a background value of ~70
451 ppbv in the BL and 60 ppbv in the FT for CO and ~30 ppbv for O₃ both in the BL and in the
452 FT.
- 453 - The Aitken to accumulation number ratio (dN_{Aitken}/dN_{Acc}), which defines the relative
454 importance of particles in the Aitken and accumulation modes. dN_{Aitken} is generally
455 associated to gas-to-particle conversion and nucleation events and is higher in fresh plumes,
456 while it decreases with the increasing of the plume lifetime due to coagulation or
457 condensation of water-soluble chemical species on the particle surface (Kulmala et al.,
458 2004).

459 The combination of $\Delta O_3/\Delta CO$ and dN_{Aitken}/dN_{Acc} has been used to retrieve additional information
460 on the atmospheric vertical structure, layering, and particle aging.

461 Within detected pollution plumes the ΔCO and ΔO_3 reach up to 100-120 ppbv and 45-55 ppbv,
462 respectively, with a corresponding $\Delta\text{O}_3/\Delta\text{CO}$ ratio which varies in the range ~ 0.10 -2.0 for all cases.
463 These values are comparable with the range of observations available in the literature for fresh and
464 moderately aged pollution plumes in the BL and in the lower FT (~ 0.2 -1.0) (Chin et al., 1994;
465 Parrish et al., 1998; Zhang et al., 2006; Cristofanelli et al., 2013). $dN_{\text{Aitken}}/dN_{\text{Acc}}$ is between about 1
466 and 20 in most of pollution cases, which indicates the presence of both fresh layers rich in Aitken
467 particles and aged plumes poor in Aitken particles. Extremely high values of $dN_{\text{Aitken}}/dN_{\text{Acc}}$ (~ 50 -
468 100-200) are measured in few cases in layers with very low dN_{Acc} concentrations.

469 The large variability in $\Delta\text{O}_3/\Delta\text{CO}$ and $dN_{\text{Aitken}}/dN_{\text{Acc}}$ indicates a strong heterogeneity in terms of
470 composition and lifetime for the different observed plumes. This heterogeneity reflects the
471 complexity in terms of sources, production processes, and transport mechanisms which
472 characterizes the Western basin. In order to illustrate this point, we have selected three examples
473 representative of different conditions observed in different areas of the basin: (i) V19, performed in
474 the Gulf of Genoa in correspondence of continental outflow events from Northern Italy/Po Valley;
475 (ii) V20, performed in Southern France during a Mistral event; (iii) V24, which measured the export
476 of pollution from the area of Barcelona. The vertical profiles of the spectral scattering coefficient σ_s ,
477 temperature T, relative humidity RH, dN_{Acc} , dN_{Aitken} , CO, O_3 , $\Delta\text{O}_3/\Delta\text{CO}$, $dN_{\text{Aitken}}/dN_{\text{Acc}}$ and wind
478 are reported in Fig. 8 for these cases.

479 *1. V19: export from northern Italy/Po Valley.* The profile shown for flight V19 (Fig. 8a) is
480 characterized by the presence of ~~two-three~~ different aerosol structures: the first one below 800 m,
481 characterized by a lower $dN_{\text{Aitken}}/dN_{\text{Acc}}$ (~ 1 -5) ~~dN_{Aitken}~~ and relatively high ~~O_3 concentrations~~
482 ~~($dN_{\text{Aitken}}/dN_{\text{Acc}} \sim 1$ -5, $\Delta\text{O}_3/\Delta\text{CO}$ (~ 0.4 -1.5)), possibly associated to moderately aged pollution, and;~~
483 the second one between 800 and 2600 m, very richer in fine particles ($dN_{\text{Aitken}}/dN_{\text{Acc}} \sim 5$ -15), so
484 possibly associated-linked to fresher emissions; and the third one above 2600 m, where the ratio
485 $dN_{\text{Aitken}}/dN_{\text{Acc}}$ rises rapidly, as will be further discussed in Sect. 5.4. The export of fresh pollution at

486 | ~~high altitudes~~800-2600 m from northern Italy as observed in V19 may be ~~associated~~related to the
487 | peculiar orography of this region and the uplift of continental air masses. This is confirmed by the
488 | analysis of the back-trajectories (Fig. 9) which indicates that the air masses arriving at 1000 and
489 | 2000 m passed over the western Po Valley at an altitude of about 400-1200 m and were then
490 | uplifted near the Ligurian coast to enter the basin above the BL. Junkermann (2009) measured high
491 | levels of fine particles up to about 2000 m in the western Po Valley, which means that the altitudes
492 | of 400-1200 m reached by our investigated air masses could have been sufficient for them to collect
493 | fresh emitted particles along their path. Conversely, below 800 m the air mass trajectory shows a
494 | longer subsidence over the sea surface in the troposphere which has possibly favoured the advection
495 | of more aged plumes, or the mixing with sea salts thus inducing the decrease of the $dN_{\text{Aitken}}/dN_{\text{Acc}}$
496 | ratio. It should be noted that the aerosol layer in the FT also shows relatively higher values of the
497 | $\Delta O_3/\Delta CO$ ratio ($\sim 0.6-1.0$) compared to the more aged plume in the BL. The enhanced amount of O_3
498 | in this air mass can be linked to a high concentration of volatile precursors which may have
499 | favoured the build-up of ozone during the plume evolution. In a recent work, Kaiser et al. (2014)
500 | suggest that in the Po Valley the high content of formaldehyde, also observed by Junkermann et al.
501 | (2009), may be responsible for the excess of O_3 production. Fresh layers in the FT up to $\sim 2000-$
502 | 3000 m possibly associated to pollution export from northern Italy have been also observed during
503 | flights V21 and V52 (not shown).

504 | 2. V20: export during a Mistral/Tramontane event. V20 provides an example of export during a
505 | Mistral/Tramontane event. As shown in Fig. 8b, winds from the northwest direction are measured at
506 | all altitudes during flight V20. The aerosol profile in the BL is characterized in the first ~ 400 m by
507 | the presence of a layer richer in dN_{Aitken} ($dN_{\text{Aitken}}/dN_{\text{Acc}} > 20$) and CO (100 ppbv close to the surface;
508 | CO data not available between 150 and 650 m) ~~and dN_{Aitken} ($dN_{\text{Aitken}}/dN_{\text{Acc}} > 20$)~~ possibly linked to
509 | fresh pollution, followed by the alternation of several layers characterized by a variable dN_{Aitken}
510 | ($1000-6000 \text{ cm}^{-3}$) and lower CO (~ 70 ppbv). A local minimum of dN_{Aitken} and σ_s is found at ~ 400

511 | m. For all these layers the O₃ is very low (~30-40 ppbv) and the $\Delta O_3/\Delta CO$ ratio is <0.6-0.8. At
512 | higher altitudes, between 1400 and 2000 m, we observe a layer enriched in O₃ ($\Delta O_3/\Delta CO \sim 1-2$) in
513 | correspondence of an almost aerosol-free region. This enriched ozone layer might be possibly
514 | associated to a downward transport from higher tropospheric layers, as also suggested by the back-
515 | trajectories (Fig. 9), as well as to the mixing with ozone rich layers along the air mass trajectory.
516 | Larger particles, from long-range transport of Saharan dust at latitudes below 30° N, are measured
517 | between 2000 and 3000 m, with a minimum of O₃ (~15-20 ppbv) registered within the layer.
518 | Several other flights were performed during Mistral/Tramontane episodes (V27, V28, V30, V32)
519 | and show, similarly to V20, the presence of several layers both in the BL and the FT.

520 | 3. V24: export from the Barcelona area. Measurements during V24 may be taken as representative
521 | of local recirculation (Pérez et al., 2004). In the V24 profile in Fig. 8c we may recognize up to 5
522 | different aerosol layers. A first layer at <200 m within the MABL, coming from the southwest and
523 | directly exported from the area of Barcelona. The layer is characterized by high CO (90-120 ppbv),
524 | and relatively low values of dN_{Aitken} (~4000 scm^{-3}) and O₃ (~50 ppbv), which possibly suggest the
525 | mixing of pollution with marine particles close to the sea surface. A second layer of fresher
526 | particles, always coming from the southwestern ern direction, is observed above the MABL between
527 | 200 and 600 m ($dN_{Aitken} \sim 6000-8000 \text{ } scm^{-3}$, O₃ ~70 ppb, with $dN_{Aitken}/dN_{Acc} \sim 5-15$, and
528 | $\Delta O_3/\Delta CO \sim 0.8-1.5$). A third, more aged, sublayer ($dN_{Aitken}/dN_{Acc} \sim 2-5$, $\Delta O_3/\Delta CO \sim 0.8-1.0$) is
529 | observed within the BL between 600 and 1000 m. The FT is characterized by the presence of
530 | moderately aged plumes from ~1000 to 2800 m ($dN_{Aitken}/dN_{Acc} \sim 2-10$, $\Delta O_3/\Delta CO \sim 0.2-0.8$), and a
531 | very aged plume at 2800-3800 m almost deprived in Aitken particles and richer in O₃
532 | ($dN_{Aitken}/dN_{Acc} < 1$, $\Delta O_3/\Delta CO \sim 0.6-1.5$). A marked local minimum is observed at the top of the BL
533 | for σ_s , dN_{Acc} , dN_{Aitken} , CO, and O₃, suggesting the presence of air masses with different origin
534 | between the BL and the FT. This is also confirmed by the analysis of the back-trajectories (Fig. 9)
535 | which indicates a low level air masses coming from the Spanish coasts in the BL, and air masses

536 travelling at higher altitudes in the FT. In particular, the layer at 2800-3800 m is possibly associated
537 to an intercontinental transport from Northern America, as shown in the trajectory ending at 3500
538 m. A similar structure characterized by the alternation of fresher and more aged plumes in the BL
539 and FT is also observed in V25 for which aerosol layers are detected up to 4000 m altitude.
540 The detailed analysis of these three events evidences the complexity of the atmospheric structure
541 over the Western Mediterranean basin in link with the different dynamical processes involved.

542

543 **5.4 Layers with enhanced Aitken mode particle numbers**

544 Isolated layers with $dN_{\text{Aitken}} \sim 10000-15000 \text{ scm}^{-3}$ have been observed ~~in few cases~~ occasionally both
545 in the BL and in the FT. The vertical profiles of dN_{Aitken} ~~only~~ for some selected cases are shown in
546 Fig. 10.

547 For about half of the observed events (~~V16 at ~200-400 m, V21 at ~400-800 m, V28 at ~250 m, and~~
548 ~~V31 at ~1000-3000 m; only V28 and V31 shown in Fig. 10~~) the dN_{Aitken} layer ~~presents a good~~
549 ~~correlation~~ appears related ~~with~~ to a simultaneous increase in dN_{Acc} , CO, and O_3 , which suggests
550 that the layer has been transported from a region directly emitting in this size range. These cases
551 are: V16 at ~200-400 m, V21 at ~400-800 m, V28 at ~250 m, and V31 at ~1000-3000 m (only V28
552 and V31 are shown in Fig. 10). The most remarkable example is ~~The most remarkable example is~~
553 V31 (Fig. 10a), performed close to the coasts of Spain near Valencia, for which ~~for which~~ the high
554 dN_{Aitken} layer extends from the top of the BL to ~3000 m altitude. The wind vector and the back-
555 trajectories (not shown) indicates that the air mass comes from the western-southwestern direction
556 above 1000 m, so the dN_{Aitken} layer can be directly related to pollution export from the urban region
557 of Valencia.

558 ~~In~~ In all the other cases the high dN_{Aitken} layer ~~appears~~ is generally not related to simultaneous dN_{Acc}
559 and O_3 increase. Two of these cases (V16 at ~800-1000 m and V28 at ~100 m) occur in the BL.

560 For the V28 layer (Fig. 10b) the dN_{Aitken} is correlated with CO which might indicate the influence of
561 local emissions close to the surface level (i.e., ship emissions). CO values are relatively high (140-
562 160 ppbv) within the layer. It has been often assumed that new particle formation events (NPF) only
563 occur in almost clean environments (e.g., O'Dowd et al., 2010; Sellegri et al., 2010), and that they
564 are suppressed under polluted conditions. In a recent study, Brines et al. (2014) show the occurrence
565 of NPF events also in urban areas with high level of pollution in the Mediterranean region. So, we
566 explore the possibility of NPF in our observations. Given the size ranges of the CPC and PCASP,
567 however, we cannot discriminate within dN_{Aitken} the particle concentration in the sole 4-20 nm
568 range, i.e. the size range involved in nucleation. So it is not possible to directly associate the V28
569 observations to NPF. In order to obtain a qualitative indication of the possible occurrence of NPF,
570 we have looked at the air mass dynamics within the layer. Several studies suggest, in fact, that NPF
571 might be favoured by turbulence and air mass mixing (e.g., Nilsson et al., 2001; Wehner et al.,
572 2010). We have thus looked at the gradient Richardson number (Ri) which gives information on the
573 atmospheric dynamical stability. Vertical profiles of Ri are also shown in Fig. 10. For V28 the
574 vertical profile of Ri indicates that below 200 m the Ri number is consistently below zero, which
575 suggests well established turbulent conditions possibly favouring NPF in this layer.

576 In other two cases (V19, Fig. 10c, and V26, Fig. 10d), under lower pollution conditions ($\text{CO} < 100$),
577 we measured high dN_{Aitken} concentration in correspondence of low dN_{Acc} layers in the FT at ~2800-
578 3000 m for V19 and 3500-4500 m for V26. For V19 and V26 layers, dN_{Aitken} seems anticorrelated
579 to CO. Also in this case the Richardson number is below Ri_{crit} in correspondence of the Aitken peak
580 meaning that conditions are favorable for turbulence within the layer, and this may indicate also in
581 this case the possible role of NPF.

582 Finally, a case of high dN_{Aitken} concentration has been also observed in correspondence of dust
583 particles between ~3000 and 4000 m (V23b, Fig. 10e). This layer can be possibly linked to the

584 photochemically-induced nucleation which may occur in presence of dust and SO₂ as hypothesised
585 in a recent study by Dupart et al. (2012) and observed by Nie et al. (2014).

586

587 **6. Conclusions**

588 The data presented in this paper gives an overview of the distribution of aerosols and trace gases
589 within the tropospheric column up to 5000 m above the Western Mediterranean basin.

590 These data add to the very few available measurements of aerosol and trace gases vertical profiles
591 over the sea surface in the Central (e.g., Junkermann, 2001; Meloni et al., 2003; Di Iorio et al.,
592 2003; Pace et al., 2014) and Eastern (e.g., Formenti et al., 2002; Dulac and Chazette, 2003) parts of
593 the basin thus contributing to improve the description of the atmospheric composition and structure
594 over the whole Mediterranean area.

595 Observations from the present study indicate that continental pollution strongly affects the
596 composition and structure of the Western Mediterranean basin both close to coastal regions and in
597 the open sea. Pollution layers extend up to 250 km far from the coasts and reach up to 3000-4000 m
598 altitude, presenting a complex and highly stratified structure. The measured particle concentration is
599 comparable with the values reported for continental Europe (Petzold et al., 2002; Junkermann,
600 2009; Hamburger et al., 2012). ~~In addition, the geographical distribution of aerosols and trace gases
601 observed in this study appears quite homogeneous within the investigated area, suggesting a
602 relatively similar contribution from the various sources located around the north-western basin.~~

603 Pollution plumes with different compositions, origins, and lifetimes are observed in link with the
604 different observed dynamical export conditions and meteorological regimes. The aerosol and trace
605 gas observations during TRAQA and SAFMED are consistent with the results of former campaigns
606 and with the interpretation of observed or well known air-masses dynamics and meteorological

607 phenomena that can occur in the Western basin (Flamant and Pelon, 1996; Millan et al., 1997;
608 Gangoiti et al., 2001; Pérez et al., 2004; Mallet et al., 2005).

609 The large heterogeneity in aerosol compositions, origins, and lifetimes as documented in this study
610 can reflect in a large heterogeneity of aerosol optical properties, with consequences for their direct
611 radiative effect in this part of the basin. This aspect will be investigated in a companion paper
612 analysing the TRAQA and SAFMED in situ measurements of the aerosol absorption and scattering
613 properties and their variability.

614 From the present observations, it is also interesting to note the relatively high values of dN_{Aitken}
615 measured both in the BL and the FT, which evidences the important contribution of ultrafine
616 particles at all altitudes over the basin. These can be linked to the different export mechanisms
617 previously discussed, as well as the possible occurrence of NPF events. Aitken particle profiles are
618 very rare over the sea surface in the Mediterranean (e.g., Junkermann et al. 2001; Pace et al.,
619 [2014](#)[2015](#)) and data comparison is quite difficult. Few studies have observed NPF in the FT in
620 continental areas (Boulon et al., 2010; Rose et al., 2014) and suggest that the export of pollution
621 into the upper troposphere, as it is common in the Western basin, might promote the occurrence of
622 these events. The observations of the present study may thus also have very large implications due
623 to the crucial role of NPF in controlling the atmospheric cloud condensation nuclei concentration
624 (Spracklen et al., 2008) and the associated aerosol indirect effect on climate.

625

626 **Author contributions**

627 J.-L.A., F.R., G.A., M.B., A.B., P.F. and K.S. designed the TRAQA and SAFMED experiments and
628 coordinated the campaigns. C.G., N.G., and C.D.B operated the instruments on board the ATR-42
629 during the flights. C.D.B. performed the data analysis with contributions from L.D., P.F., F.R.,
630 A.B., G.A., J.-C.R., and M.B.. G.A. performed the FLEXTRA simulations. J.-C.R. performed the
631 WRF-Chem simulations. C.D.B. wrote the manuscript.

632

633 **Acknowledgements**

634 All measurement presented here are from the Chemistry-Aerosol Mediterranean Experiment project
635 (ChArMEx, <http://charmex.lsce.ipsl.fr>), which is the atmospheric component of the French
636 multidisciplinary program MISTRALS (Mediterranean Integrated Studies at Regional And Local
637 Scales). ChArMEx-France was principally funded by INSU, ADEME, ANR, CNES, CTC (Corsica
638 region), EU/FEDER, Météo-France, and CEA. TRAQA was funded by ADEME/PRIMEQUAL and
639 MISTRALS/ChArMEx programmes and Observatoire Midi-Pyrénées. SAFMED was funded by the
640 ANR project SAF-MED (Secondary Aerosol Formation in the MEDiterranean, [grant SIMI6 ANR-
641 12-BS06-0013](#)). C. Di Biagio thanks the Centre National des Etudes Spatiales (CNES) for financial
642 support.

643 The authors wish to thank the technicians, pilots and ground crew of SAFIRE (Service des Avions
644 Français Instruments pour la Recherche en Environnement) for facilitating the instrument
645 integration and conducting flying operations. We thank S. Chevaillier, L. Girault, R. Loisil, J.
646 Pelon, S. Triquet, and P. Zapf for their contribution during the campaigns. We thank S. Basart, J.
647 M. Baldasano, M. Mallet, P. Goloub, J. Piazzola and their staff for establishing and maintaining the
648 Barcelona, Ersar, and Frioul AERONET sites. Helpful discussions with G. Pace are gratefully
649 acknowledged.

650 [We thank also two anonymous reviewers whose suggestions helped to clarify the manuscript.](#)

651

652 **References**

- 653 Ancellet, G. and Ravetta, F.: Analysis and validation of ozone variability observed by lidar during
654 the ESCOMPTE-2001 campaign, *Atmos. Res.*, 74, 435–459, 2005.
- 655 Anderson, T. L., Covert, D. S., Marshall, S. F., Laucks, M. L., Charlson, R. J., Waggoner, A. P.,
656 Ogren, J. A., Caldow, R., Holm, R. L., Quant, F. R., Sem, G. J., Wiedensholler, A., Ahlquist, N.
657 A., and Bates, T. S.: Performance characteristics of a high-sensitivity, three-wavelength, total
658 scatter/backscatter nephelometer, *J. Atmos. Ocean. Tech.*, 13, 967–986, 1996.

- 659 Anderson, T. L. and Ogren, J. A.: Determining aerosol radiative properties using the TSI 3563
660 integrating nephelometer, *Aerosol Sci. Technol.*, 29, 57–69, 1998.
- 661 Bonasoni, P., Cristofanelli, P., Calzolari, F., Bonafè, U., Evangelisti, F., Stohl, A., Zauli Sajani, S.,
662 van Dingenen, R., Colombo, T., and Balkanski, Y.: Aerosol-ozone correlations during dust
663 transport episodes, *Atmos. Chem. Phys.*, 4, 1201-1215, doi:10.5194/acp-4-1201-2004, 2004.
- 664 Boucher, O., Randall, D., Artaxo, P., Bretherton, C., Feingold, G., Forster, P., Kerminen, V.-M.,
665 Kondo, Y., Liao, H., Lohmann, U., Rasch, P., Satheesh, S. K., Sherwood, S., Stevens, B., and
666 Zhang, X. Y.: Clouds and Aerosols. In: *Climate Change 2013: The Physical Science Basis. Contribution of Working Group I to the Fifth Assessment Report of the Intergovernmental Panel on Climate Change* [Stocker, T.F., D. Qin, G.-K. Plattner, M. Tignor, S.K. Allen, J. Boschung, A. Nauels, Y. Xia, V. Bex and P.M. Midgley (eds.)]. Cambridge University Press, Cambridge, United Kingdom and New York, NY, USA, 571-657, 2013.
- 671 Boulon, J., Sellegri, K., Venzac, H., Picard, D., Weingartner, E., Wehrle, G., Collaud Coen, M.,
672 Bütikofer, R., Flückiger, E., Baltensperger, U., and Laj, P.: New particle formation and ultrafine
673 charged aerosol climatology at a high altitude site in the Alps (Jungfraujoch, 3580 m a.s.l.,
674 Switzerland), *Atmos. Chem. Phys.*, 10, 9333–9349, doi: 10.5194/acp-10-9333-2010, 2010.
- 675 Brines, M., Dall'Osto, M., Beddows, D. C. S., Harrison, R. M., Gómez-Moreno, F., Núñez, L.,
676 Artíñano, B., Costabile, F., Gobbi, G. P., Salimi, F., Morawska, L., Sioutas, C., and Querol, X.:
677 Frequency of new particle formation events in the urban Mediterranean climate, *Atmos. Chem. Phys. Discuss.*, 14, 26463-26494, doi:10.5194/acpd-14-26463-2014, 2014.
- 679 Chazette, P., Randriamiarisoa, H., Sanak, J., Couvert, P., and Flamant, C.: Optical properties of
680 urban aerosol from airborne and ground based in situ measurements performed during the
681 ESQUIF program, *J. Geophys. Res.*, 110, D02206, doi:10.1029/2004JD004810, 2005.
- 682 Chin, M., Jacob, D. J., Munger, J. W., Parrish, D. D., and Doddridge, B. G.: Relationship of ozone
683 and carbon monoxide over North America, *J. Geophys. Res.*, 99, 14,565–14,573, 1994.
- 684 Colette, A., Ancellet, G., Menut, L., and Arnold, S. R.: A Lagrangian analysis of the impact of
685 transport and transformation on the ozone stratification observed in the free troposphere during
686 the ESCOMPTE campaign, *Atmos. Chem. Phys.*, 6, 3487-3503, doi:10.5194/acp-6-3487-2006,
687 2006.
- 688 Cristofanelli, P., Fierli, F., Marinoni, A., Calzolari, F., Duchi, R., Burkhart, J., Stohl, A., Maione,
689 M., Arduini, J., and Bonasoni, P.: Influence of biomass burning and anthropogenic emissions on
690 ozone, carbon monoxide and black carbon at the Mt. Cimone GAW-WMO global station (Italy,
691 2165 m a.s.l.), *Atmos. Chem. Phys.*, 13, 15–30, 2013.
- 692 Di Iorio, T., di Sarra, A., Junkermann, W., Cacciani, M., Fiocco, G., and Fua`, D.: Tropospheric
693 aerosols in the Mediterranean: 1. Microphysical and optical properties, *J. Geophys. Res.*,
694 108(D10), 4316, doi:10.1029/2002JD002815, 2003.
- 695 Drobinski, P, Saïd, F., Ancellet, G., Arteta, J. Augustin, P., Bastin, S., Brut, A., Caccia, J. L.,
696 Campistron, B., Cautenet, S., Colette, A., Coll, I., Corsmeier, U., Cros, B., Dabas, A., Delbarre,
697 H., Dufour, A., Durand, P., Guénard, V., Hasel, M., Kalthoff, N., Kottmeier, C., Lasry, F.,
698 Lemonsu, A., Lohou, F., Masson, V., Menut, L., Moppert, C., Peuch, V. H., Puygrenier, V.,
699 Reitebuch, O., and Vautard, R.: Regional transport and dilution during high-pollution episodes in
700 southern France: Summary of findings from the Field Experiment to Constraint Models of
701 Atmospheric Pollution and Emissions Transport (ESCOMPTE), *J. Geophys. Res.*, 112, D13105,
702 doi:10.1029/2006JD007494, 2007.

- 703 Dulac, F., and Chazette, P.: Airborne study of a multi-layer aerosol structure in the eastern
704 Mediterranean observed with the airborne polarized lidar ALEX during a STAAARTE campaign
705 (7 June 1997), *Atmos. Chem. Phys.*, 3, 1817–1831, doi:10.5194/acp-3-1817-2003, 2003.
- 706 Dupart, Y.; King, S. M., Nekat, B., Nowak, A., Wiedensohler, A., Herrmann, H., David, G.,
707 Thomas, B., Miffre, A., Rairoux, P., D'Anna, B., and George, C.: Mineral dust photochemistry
708 induces nucleation events in the presence of SO₂. *PNAS*, 109, (51), 20842–20847, 2012.
- 709 Ebert, M., Weinbruch, S., Rausch, A., Gorzawski, G., Hoffmann, P., Wex, H., and Helas, G.: The
710 complex refractive index of aerosols during LACE 98 as derived from the analysis of individual
711 particles, *J. Geophys. Res.*, 107, D21, 8121, doi:10.1029/2000JD000195, 2002.
- 712 Ebert, M., Weinbruch, S., Hoffmann, P., and Ortner, H. M.: The chemical composition and complex
713 refractive index of rural and urban influenced aerosols determined by individual particle
714 analysis, *Atmos. Environ.*, 38, 6531–6545, 2004.
- 715 Flamant, C., and Pelon, J.: Atmospheric boundary-layer structure over the Mediterranean during a
716 Tramontane event, *Quart. J. Roy. Meteorol. Soc.*, 122, 1741–1778, 1996.
- 717 Formenti, P., Reiner, T., Sprung, D., Andreae, M. O., Wendisch, M., Wex, H., Kindred, D., Dewey,
718 K., Kent, J., Tzortziou, M., Vasaras, A., and Zerefos, C.: STAAARTE-MED 1998 summer
719 airborne measurements over the Aegean Sea, 1, Aerosol particles and trace gases, *J. Geophys.
720 Res.*, 107, D21, doi:10.1029/2001JD001337, 2002.
- 721 Formenti, P., Rajot, J. L., Desboeufs, K., Saïd, F., Grand, N., Chevaillier, S., and Schmechtig, C.:
722 Airborne observations of mineral dust over western Africa in the summer Monsoon season:
723 spatial and vertical variability of physico-chemical and optical properties, *Atmos. Chem. Phys.*,
724 11, 6387–6410, doi:10.5194/acp-11-6387-2011, 2011.
- 725 Gangoiti, G., M. M. Millán, R. Salvador, E. Mantilla: Long-Range transport and recirculation of
726 pollutants in the Western Mediterranean during the RECAPMA Project. *Atmos. Environ.*, 35,
727 6267–6276, 2001.
- 728 Gkikas, A., Houssos, E. E., Hatzianastassiou, N., Papadimas, C. D., and Bartzokas, A.: Synoptic
729 conditions favouring the occurrence of aerosol episodes over the broader Mediterranean basin,
730 *Q. J. R. Meteorol. Soc.*, 138: 932–949. doi:10.1002/qj.978, 2012.
- 731 Grell, G. A., Peckham, S. E., Schmitz, R., McKeen, S. A., Frost, G., Skamarock, W. C., and Eder,
732 B.: Fully coupled “online” chemistry within the WRF model, *Atmos. Environ.*, 39, 6957–6975,
733 2005.
- 734 Hamburger, T., McMeeking, G., Minikin, A., Petzold, A., Coe, H., and Krejci, R.: Airborne
735 observations of aerosol microphysical properties and particle ageing processes in the troposphere
736 above Europe, *Atmos. Chem. Phys.*, 12, 11533–11554, doi:10.5194/acp-12-11533-2012, 2012.
- 737 Haywood, J., Johnson, B., Osborne, S., Mulcahy, J., Brooks, M., Harrison, M., Milton, S., and
738 Brindley, H.: Observations and modelling of the solar and terrestrial radiative effects of Saharan
739 dust: a radiative closure case-study over oceans during the GERBILS campaign, *Q. J. R.
740 Meteorol. Soc.*, 137, 1211–1226, doi:10.1002/qj.770, 2011.
- 741
- 742 [Highwood, E. J., Northway, M. J., McMeeking, G. R., Morgan, W. T., Liu, D., Osborne, S.,](#)
743 [Bower, K., Coe, H., Ryder, C., and Williams, P.: Aerosol scattering and absorption during the](#)
744 [EUCAARI-LONGREX flights of the Facility for Airborne Atmospheric Measurements \(FAAM\)](#)
745 [BAe-146: can measurements and models agree?, *Atmos. Chem. Phys.*, 12, 7251–7267,](#)
746 [doi:10.5194/acp-12-7251-2012, 2012.](#)

- 747 [Holben, B. N., Eck, T. F., Slutsker, I., Tanré, D., Buis, J. P., Setzer, A., Vermote, E., Reagan, J. A.,](#)
748 [Kaufman, Y., Nakajima, T., Lavenu, F., Jankowiak, I., and Smirnov, A.: AERONET: a federated](#)
749 [instrument network and data archive for aerosol characterization, *Rem. Sens. Environ.*, 66, 1–16,](#)
750 [1998.](#)
- 751 Jiménez, P., Pérez, C., Rodríguez, A., and Baldasano, J. M. : Correlated levels of particulate matter
752 and ozone in the western Mediterranean basin: Air quality and lidar measurements, 22nd Annual
753 Conference Am. Assoc. for Aerosol Res., Anaheim, California, 20-24 October 20-24 2003,
754 2003.
- 755 Jiménez, P., Lelieveld, J., and Baldasano, J. M.: Multiscale modeling of air pollutants dynamics in
756 the northwestern Mediterranean basin during a typical summertime episode, *J. Geophys. Res.*,
757 111, D18306, doi:10.1029/2005JD006516, 2006.
- 758 Jiménez-Guerrero, P., Jorba, O., Baldasano, J. M., and Gassó, S.: The use of a modelling system as
759 a tool for air quality management: Annual high-resolution simulations and evaluation, *Sci. Tot.*
760 *Environ.*, 390, 323–340, 2008.
- 761 Junkermann, W.: An ultralight aircraft as platform for research in the lower troposphere: System
762 performance and first results from radiation transfer studies in stratiform aerosol layers and
763 broken cloud conditions, *J. Atmos. Oceanic Technol.*, 18, 934–946, 2001.
- 764 Junkermann, W.: On the distribution of formaldehyde in the western Po-Valley, Italy, during 800
765 FORMAT 2002/2003, *Atmos. Chem. Phys.*, 9, 9187-9196, doi:10.5194/acp-9-9187-2009, 2009.
- 766 Kaiser, J., Wolfe, G. M., Bohn, B., Broch, S., Fuchs, H., Ganzeveld, L. N., Gomm, S., Häsel, R.,
767 Hofzumahaus, A., Holland, F., Jäger, J., Li, X., Lohse, I., Lu, K., Rohrer, F., Wegener, R.,
768 Mentel, T. F., Kiendler-Scharr, A., Wahner, A., and Keutsch, F. N.: Evidence for an unidentified
769 ground-level source of formaldehyde in the Po Valley with potential implications for ozone
770 production, *Atmos. Chem. Phys. Discuss.*, 14, 25139-25165, doi:10.5194/acpd-14-25139-2014,
771 2014.
- 772 Kallos, G., Astitha, M., Katsafados, P., and Spyrou, C.: Long-range transport of anthropogenically
773 and naturally produced particulate matter in the Mediterranean and North Atlantic: Current state
774 of knowledge, *J. Appl. Meteorol. Climatol.*, 46, 1230–1251, 2007.
- 775 Kulmala, M., Vehkamäki, H., Petaja, T., Dal Maso, M., Lauri, A., Kerminen, V.-M., Birmili, W.,
776 and McMurry, P.H.: Formation and growth rates of ultrafine atmospheric particles: A review of
777 observations, *J. Aerosol Sci.*, 35(2), 143–176, 2004.
- 778 Lelieveld, J., Berresheim, H., Borrmann, S., Crutzen, P. J., Dentener, F. J., Fischer, H., Feichter, J.,
779 Flatau, P. J., Heland, J., Holzinger, R., Kormann, R., Lawrence, M. G., Levin, Z., Markowicz,
780 K. M., Mihalopoulos, N.; Minikin, A., Ramanathan, V., de Reus, M., Roelofs, G. J., Scheeren,
781 H. A., Sciare, J., Schlager, H., Schultz, M., Siegmund, P., Steil, B., Stephanou, E. G., Stier, P.,
782 Traub, M., Warneke, C., Williams, J., and Ziereis H.: Global air pollution crossroads over the
783 Mediterranean, *Science*, 298, 794–799, doi:10.1126/science.1075457, 2002.
- 784 Liu, Y. and Daum, P.: The effect of refractive index on size distributions and light scattering
785 coefficients derived from optical particle counters, *J. Aerosol Sci.*, 31, 945–957, 2000.
- 786 Mallet, M., Roger, J. C., Despiiau, S., Dubovik, O., and Putaud, J. P.: Microphysical and optical
787 properties of aerosol particles in urban zone during ESCOMPTE, *Atmos. Res.*, 69, 73–97, 15
788 2003.
- 789 Mallet, M., Van Dingenen, R., Roger, J. C., Despiiau, S., and Cachier, H.: In situ airborne
790 measurements of aerosol optical properties during photochemical pollution events, *J. Geophys.*
791 *Res.*, 110, D03205, doi:10.1029/2004JD005139, 2005.

- 792 Mallet, M., Gomes, L., Solmon, F., Sellegri, K., Pont, V., Roger, J. C., Missamou, T., and Piazzola,
793 J.: Calculation of key optical properties of the main anthropogenic aerosols over the Western
794 French coastal Mediterranean Sea, *Atmos. Res.*, 101, 396–411, 2011.
- 795 Meloni, D., di Sarra, A., DeLuisi, J., Di Iorio, T., Fiocco, G., Junkermann, W., and Pace, G.:
796 Tropospheric aerosols in the Mediterranean: 2. Radiative effects through model simulations and
797 measurements, *J. Geophys. Res.*, 108(D10), 4317, doi:10.1029/2002JD002807, 2003.
- 798 Millán, M., Salvador, R., Mantilla, E., and Artinãno, B.: Meteorology and photochemical air
799 pollution in Southern Europe: experimental results from EC research projects, *Atmos. Environ.*,
800 30 (12), 1909–1924, 1996.
- 801 Millan, M. M., Salvador, R., Mantilla, E., and Kallos, G.: Photooxidant dynamics in the Western
802 Mediterranean in summer: Results from European research projects, *J. Geophys. Res.*, 102(D7),
803 8811–8823, 1997.
- 804 Millán, M. M., Mantilla, E., Salvador, R., Carratala, A., Sanz, M. J., Alonso, L., Gangoiti, G., and
805 Navazo, M.: Ozone cycles in the western Mediterranean basin: interpretation of monitoring data
806 in complex terrain, *J. Appl. Meteorol.*, 4, 487–507, 2000.
- 807 Monks, P., Granier, C., Fuzzi, S., Stohl, A., Williams, M., Akimoto, H., Amann, M., Baklanov, A.,
808 Baltensperger, U., Bey, I., Blake, N., Blake, R., Carslaw, K., Cooper, O., Dentener, F., Fowler,
809 D., Fragkou, E., Frost, G., Generoso, S., Ginoux, P., Grewe, V., Guenther, A., Hansson, H.,
810 Henne, S., Hjorth, J., Hofzumahaus, A., Huntrieser, H., Isaksen, I., Jenkin, M., Kaiser, J.,
811 Kanakidou, M., Klimont, Z., Kulmala, M., Laj, P., Lawrence, M., Lee, J., Liousse, C., Maione,
812 M., McFiggans, G., Metzger, A., Mieville, A., Moussiopoulos, N., Orlando, J., O’Dowd, C.,
813 Palmer, P., Parrish, D., Petzold, A., Platt, U., Pöschl, U., Prévôt, A., Reeves, C., Reimann, S.,
814 Rudich, Y., Sellegri, K., Steinbrecher, R., Simpson, D., ten Brink, H., Theloke, J., van der Werf,
815 G., Vautard, R., Vestreng, V., Vlachokostas, C., and von Glasow, R.: Atmospheric composition
816 change – global and regional air quality, *Atmos. Environ.*, 43, 5268–5350,
817 doi:10.1016/j.atmosenv.2009.08.021, 2009.
- 818 Müller, D., Ansmann, A., Wagner, F., Franke, K., and Althausen, D.: European pollution outbreaks
819 during ACE 2: Microphysical particle properties and single-scattering albedo inferred from
820 multiwavelength lidar observations, *J. Geophys. Res.*, 107, D15, 4248, 10.1029/2001JD001110,
821 2002.
- 822 Nedélec, P., Cammas, J.-P., Thouret, V., Athier, G., Cousin, J.-M., Legrand, C., Abonnel, C.,
823 Lecoœur, F., Cayez, G., and Marizy, C.: An improved infrared carbon monoxide analyser for
824 routine measurements aboard commercial Airbus aircraft: technical validation and first scientific
825 results of the MOZAIC III programme, *Atmos. Chem. Phys.*, 3, 1551–1564, doi:10.5194/acp-3-
826 1551-2003, 2003.
- 827 Nie, W., Ding, A., Wang, T., Kerminen, V.-M., George, C., Xue, L., Wang, W., Zhang, Q., Petaja,
828 T., Qi, X., Gao, X., Wang, X., Yang, X., Fu, C., and Kulmala, M.: Polluted dust promotes new
829 particle formation and growth, *Sci. Rep.*, 4, 6634, doi:10.1038/srep06634, 2014.
- 830 Nilsson, E. D., Rannik, U., Kulmala, M., Buzorius, G., and O’Dowd, C. D.: Effects of continental
831 boundary layer evolution, convection, turbulence and entrainment, on aerosol formation,
832 *TellusB*, 53, 441–461, 2001.
- 833 O’Dowd, C., Monahan, C., and Dall’Osto, M.: On the occurrence of open ocean particle production
834 and growth events, *Geophys. Res. Lett.*, 37, L19805, doi:10.1029/2010GL044679, 2010.
- 835 Pace, G., di Sarra, A., Meloni, D., Piacentino, S., and Chamard, P.: Aerosol optical properties at
836 Lampedusa (Central Mediterranean). 1. Influence of transport and identification of different
837 aerosol types, *Atmos. Chem. Phys.*, 6, 697–713, doi:10.5194/acp-6-697-2006.

- 838 Pace, G., Junkermann, W., Vitali, L., di Sarra, A., Meloni, D., Cacciani, M., Cremona, G.,
839 Iannarelli, A. M., and Zanini, G: On the complexity of the boundary layer structure and aerosol
840 vertical distribution in the coastal Mediterranean regions: a sea breeze, desert dust transport, and
841 free-tropospheric air intrusion case study in Southern, submitted to TellusB, [20142015](#).
- 842 Parrish, D. D., Holloway, J. S., Trainer, M., Murphy, P. C., Fehsenfeld, F. C., and Forbes, G. L.:
843 Export of North America ozone pollution to the North Atlantic Ocean, *Science*, 259, 1436–1439,
844 1993.
- 845 Parrish, D. D., Trainer, M., Holloway, J. S., Yee, J. E., Warshawsky, M. S., Fehsenfeld, F. C.,
846 Forbes, G. L., and Moody, J. L.: Relationships between ozone and carbon monoxide at surface
847 sites in the North Atlantic region, *J. Geophys. Res.*, 103, 13,357– 13,376, 1998.
- 848 Pérez, C., Sicard, M., Jorba, O., Comeron, A., and Baldasano, J. M.: Summertime re-recirculations
849 of air pollutants over the North-Eastern Iberian coast observed from systematic EARLINET lidar
850 measurements in Barcelona, *Atmos. Environ.*, 38, 3983–4000, 2004.
- 851 Pérez, N., Pey, J., Castillo, S., Viana, M., Alastuey, A., and Querol, X.: Interpretation of the
852 variability of levels of regional background aerosols in the Western Mediterranean, *Sci. Tot.*
853 *Environ.*, 407, 527–540, 2008.
- 854 Petzold, A., Fiebig, M., Flentje, H., Keil, A., Leiterer, U., Schroder, F., Stifter, A., Wendisch, M.,
855 and Wendling, P.: Vertical variability of aerosol properties observed at a continental site during
856 the Lindenberg Aerosol Characterization Experiment (LACE 98), *J. Geophys. Res.*, 107, 8128,
857 doi:10.1029/2001JD001043, 2002.
- 858 Pey, J., Querol, X., and Alastuey, A.: Discriminating the regional and urban contributions in the
859 North-Western Mediterranean: PM levels and composition, *Atmos Environ*, 44, 1587–96, 2010.
- 860 Raut, J.-C., and Chazette, P.: Vertical profiles of urban aerosol complex refractive index in the
861 frame of ESQUIF airborne measurements, *Atmos. Chem. Phys.*, 8, 901–919, 2008.
- 862 Rose, C., Sellegri, K., Asmi, E., Hervo, M., Freney, E., Junninen, H., Duplissy, J., Sipilä, M.,
863 Kontkanen, J., Lehtipalo, K., and Kulmala, M.: Major contribution of neutral clusters to new
864 particle formation in the free troposphere, *Atmos. Chem. Phys. Discuss.*, 14, 18355–18388,
865 2014.
- 866 Salameh, T., Drobinski, P., Menut, L., Bessagnet, B., Flamant, C., Hodzic, A., and Vautard, R.:
867 Aerosol distribution over the western Mediterranean basin during a Tramontane/Mistral event,
868 *Ann. Geophys.*, 25, 2271–2291, 2007.
- 869 Sellegri, K., Laj, P., Venzac, H., Boulon, J., Picard, D., Villani, P., Bonasoni, P., Marinoni, A.,
870 Cristofanelli, P., and Vuillermoz, E.: Seasonal variations of aerosol size distributions based on
871 long-term measurements at the high altitude Himalayan site of Nepal Climate Observatory-
872 Pyramid (5079 m), Nepal, *Atmos. Chem. Phys.*, 10, 10679–10690, doi:10.5194/acp-10-10679-
873 2010, 2010.
- 874 Soriano, C., Baldasano, J. M., Buttler, W. T., and Moore, K.: Circulatory patterns of air pollutants
875 within the Barcelona air basin in a summertime situation: lidar and numerical approaches.
876 *Bound.-Lay. Meteorol.*, 98 (1), 33–55, 2001.
- 877 Spracklen, D. V., Carslaw, K. S., Kulmala, M., Kerminen, V.-M., Sihto, S.-L., Riipinen, I.,
878 Merikanto, J., Mann, G. W., Chipperfield, M. P., and Wiedensohler, A.: Contribution of particle
879 formation to global cloud condensation nuclei concentrations, *Geophys. Res. Lett.*, 35, L06808,
880 doi:10.1029/2007GL033038, 2008.

881 Stohl, A., Wotawa, G., Seibert, P., and Krompkolb, H.: Interpolation errors in wind fields as a
882 function of spatial and temporal resolution and their impact on different types of kinematic
883 trajectories, *J. Appl. Meteorol.*, 34, 2149–2165, 1995.

884 Velchev, K., Cavalli, F., Hjorth, J., Marmer, E., Vignati, E., Dentener, F., and Raes, F.: Ozone over
885 the Western Mediterranean Sea – results from two years of shipborne measurements, *Atmos.*
886 *Chem. Phys.*, 11, 675-688, doi:10.5194/acp-11-675-2011, 2011.

887 Wallace J.M., and Hobbs, P.V.: *Atmospheric science: an introductory survey* (2nd edition).
888 International Geophysics Series 92, Academic press, Burlington, 484pp, 2006.

889 Wehner, B., H. Siebert, A. Ansmann, F. Ditas, P. Seifert, F. Stratmann, A. Wiedensohler, A. 956
890 Apituley, R. A. Shaw, H. E. Manninen, and M. Kulmala (2010), Observations of turbulence
891 induced new particle formation in the residual layer, *Atmos. Chem. Phys.*, 10, 4319–4330, 958
892 doi:10.5194/acp-10-4319-2010.

893 Wiegner, M., Emeis, S., Freudenthaler, V., Heese, B., Junkermann, W., Münkler, C., Schäfer, K.,
894 Seefeldner, M., and Vogt, S.: Mixing layer height over Munich, Germany: variability and
895 comparisons of different methodologies, *J. Geophys. Res.*, 111, D13201,
896 doi:10.1029/2005JD006593, 2006.

897 Zhang, L., Jacob, D. J., Bowman, K. W., Logan, J. A., Turquety, S., Hudman, R. C., Li, Q., Beer,
898 R., Worden, H. M., Worden, J. R., Rinsland, C. P., Kulawik, S. S., Lampel, M. C., Shephard, M.
899 W., Fisher, B. M., Eldering, A., and Avery M. A.: Ozone-CO correlations determined by the
900 TES satellite instrument in continental outflow regions, *Geophys. Res. Lett.*, 33, L18804,
901 doi:10.1029/2006GL026399, 2006.

902

903

904

905

906 **Tables**907 **Table 1.** Summary of information on the TRAQA and SAFMED flights.

908

Measurement campaign	Flight number	Date	Take off-landing time (UTC)	Departure-arrival	Geographic area investigated	<u>Description</u> Events observed
TRAQA 2012	V16	20/06/2012	13:12 – 16:34	Toulouse-Toulouse	Gulf of Lion	Test flight
	V17	22/06/2012	09:01 – 12:54	Toulouse-Toulouse	South-western France (over land) and the Atlantic Ocean	Test flight, biogenic emissions
	V18	26/06/2012	07:13 – 09:18	Toulouse-Bastia	Gulf of Genoa	Export of pollution from Northern Italy/Pô Valley, north- we easterly winds
	V19	26/06/2012	10:42 – 13:46	Bastia-Toulouse	Gulf of Genoa	Export of pollution from Northern Italy/Pô Valley, north- we easterly winds
	V20	27/06/2012	04:07 – 08:00	Toulouse-Nimes	Sea area south of Marseille/Toulon	Export of pollution during a Mistral-Tramontane event
	V21	27/06/2012	09:39 – 13:16	Nimes-Toulouse	Western coast of Corsica	Export of pollution from Northern Italy/Pô Valley, north- we easterly winds
	V22	29/06/2012	05:13 – 08:50	Toulouse-Bastia	Eastern coast of Corsica	Dust outbreak
	V23	29/06/2012	10:13 – 14:12	Bastia-Toulouse	Eastern and western coasts of Corsica	Dust outbreak
	V24	03/07/2012	13:19 – 17:12	Toulouse-Toulouse	Sea area north-east of Barcelona	Export of pollution from Barcelona, westerly/south-westerly winds
	V25	04/07/2012	07:18 – 10:54	Toulouse-Toulouse	Sea area south of Marseille/Toulon	Follow of Barcelona pollution plumes
	V26	04/07/2012	15:25 – 18:36	Toulouse-Toulouse	Gulf of Lion	Follow of Barcelona pollution plumes
	V27	06/07/2012	08:00 – 11:55	Toulouse-Toulouse	Sea area south of Marseille	Export of pollution during a moderate Mistral-Tramontane event
	V28	06/07/2012	14:01 – 17:45	Toulouse-Toulouse	Sea area south of Nice/Toulon	Export of pollution during a moderate Mistral-Tramontane event
	V29	07/07/2012	08:19 – 10:59	Toulouse-Nimes	Southern France (over land)	Biogenic emissions
	V30	07/07/2012	13:03 – 17:10	Nimes-Toulouse	Gulf of Genoa	Export of pollution during a moderate Mistral-Tramontane event
	V31	10/07/2012	13:41 – 17:21	Toulouse-Toulouse	Eastern coast of Spain	Characterization of pollution near coastal

						sources
	V32	11/07/2012	11:23 – 14:48	Toulouse-Toulouse	Southeastern coast of France and Gulf of Genoa	Characterization of pollution near coastal sources
SAFMED 2013	V46	24/07/2013	10:34 – 13:06	Genoa-Cagliari	Gulf of Genoa and eastern coast of Corsica and Sardinia	Characterization of pollution plumes in the Gulf of Genoa, Corsica, and Sardinia; westerly/south-westerly winds
	V47	24/07/2013	14:21 – 16:29	Cagliari-Genoa	Eastern coast of Corsica and Sardinia and Gulf of Genoa	Characterization of pollution plumes in the Gulf of Genoa, Corsica, and Sardinia; westerly/south-westerly winds
	V48	25/07/2013	13:12 – 16:02	Genoa-Ersa	Gulf of Genoa	Characterization of pollution in the Gulf of Genoa; westerly/south-westerly winds
	V49	27/07/2013	11:08 – 13:07	Genoa-Alghero	Central Italy (over land)	Characterization of pollution in central Italy
	V50	27/07/2013	15:33 – 16:48	Alghero-Genoa	Eastern coast of Corsica and Gulf of Genoa	Characterization of pollution plumes in the Gulf of Genoa, Corsica, and Sardinia; westerly/south-westerly winds + dust outbreak
	V51	30/07/2013	13:05 – 15:50	Genoa-Ersa	Gulf of Genoa	Characterization of pollution in the Gulf of Genoa; very low north/north-westerly winds
	V52	01/08/2013	12:03 – 15:24	Genoa-Alghero	Western coast of Corsica	Characterization of pollution in western Corsica; export of pollution from Northern Italy/Pô Valley; north-easterly winds

909
910
911
912
913
914
915
916

917 **Table 2.** Comparison of the number concentrations dN_{Aitken} (0.004-0.1 μm) and dN_{Acc} (0.1-1.0 μm)
 918 observed during the TRAQA/SAFMED field campaigns with those reported in literature for
 919 continental Europe. All literature data refer to airborne measurements.
 920

<u>Atmospheric layer</u>	<u>Parameter</u>	<u>TRAQA/SAFMED</u>	<u>Literature over continental Europe</u>
<u>Free troposphere (FT)</u>	<u>$dN_{\text{Aitken}} (\text{scm}^{-3})$</u>	<u>0-19250</u>	<u>812-9149^b; 0-980^e</u>
	<u>$dN_{\text{Acc}} (\text{scm}^{-3})$</u>	<u>34-3233</u>	<u>20-80^a; 25-85^c; 0-500^f</u>
<u>Boundary layer (BL)</u>	<u>$dN_{\text{Aitken}} (\text{scm}^{-3})$</u>	<u>4-22471</u>	<u>1037-31370^b; 1000-20000^c; 0-30000^d; 0-19000^e</u>
	<u>$dN_{\text{Acc}} (\text{scm}^{-3})$</u>	<u>90-3215</u>	<u>70-560^a; 10-50^c; 400-1200^e; 0-2000^f</u>

921
 922 ^a Petzold et al. (2002), Central Europe, July-August 1998; size range $dN_{\text{Acc}} (>0.15 \mu\text{m})$

923 ^b Mallet et al. (2005), Southeastern France, June 2001; size range $dN_{\text{Aitken}} (0.006-0.6 \mu\text{m})$

924 ^c Wiegner et al. (2006), Germany, May 2003; ; size range $dN_{\text{Aitken}} (>0.01 \mu\text{m})$, $dN_{\text{Acc}} (>0.3 \mu\text{m})$

925 ^d Junkermann (2009), Po Valley, July-August 2002 and Septmeber-October 2003; ; size range $dN_{\text{Aitken}} (>0.01 \mu\text{m})$

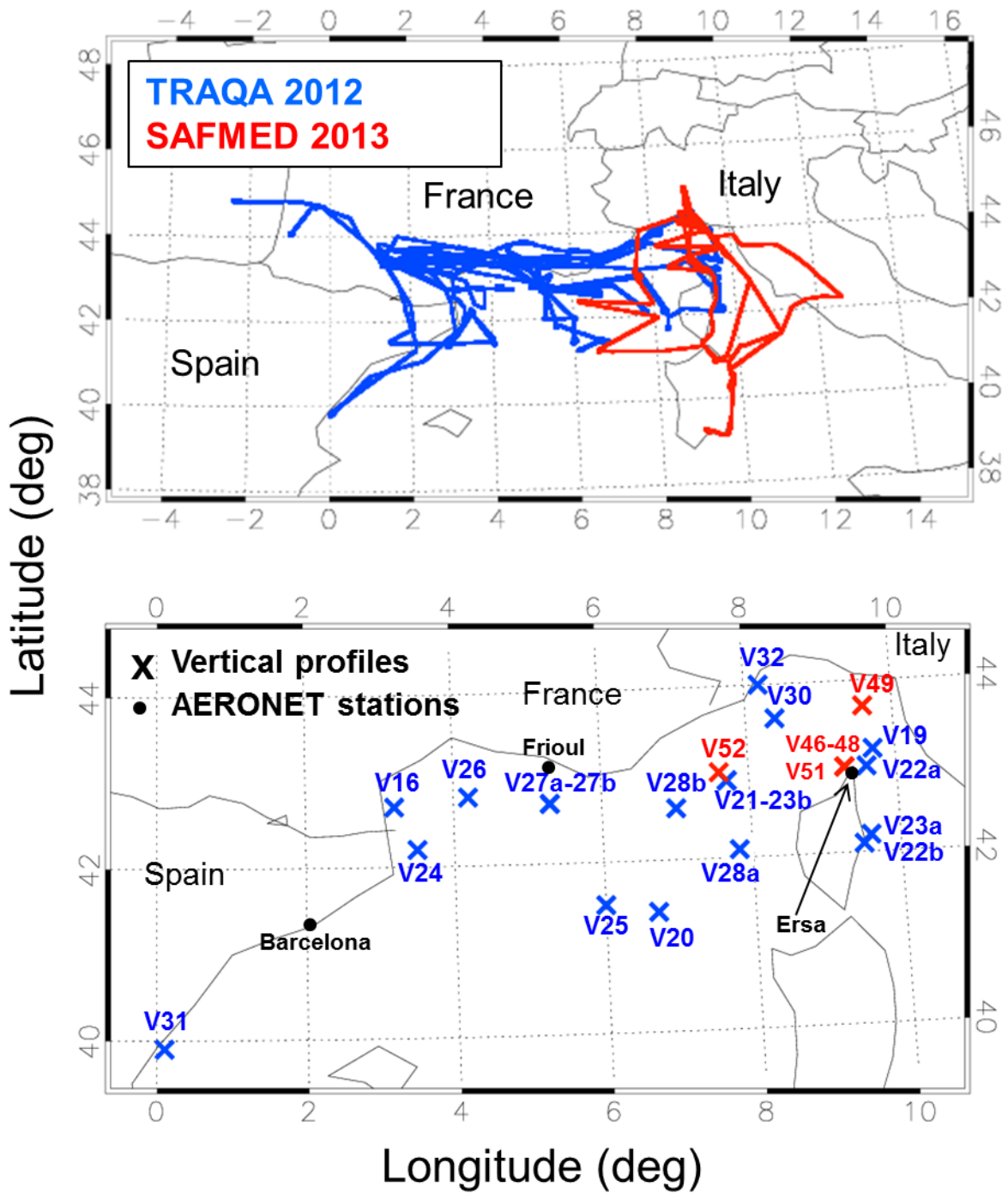
926 ^e Hamburger et al. (2012), central Europe, May 2008; size range $dN_{\text{Aitken}} (0.004-0.15 \mu\text{m})$, $dN_{\text{Acc}} (>0.15 \mu\text{m})$

927 ^f Highwood et al. (2012), central Europe, May 2008; size range $dN_{\text{Aitken}} (0.004-0.15 \mu\text{m})$, $dN_{\text{Acc}} (>0.15 \mu\text{m})$

928
 929
 930
 931
 932
 933
 934
 935
 936
 937
 938
 939
 940
 941
 942
 943
 944
 945
 946
 947
 948

949 **Figures**

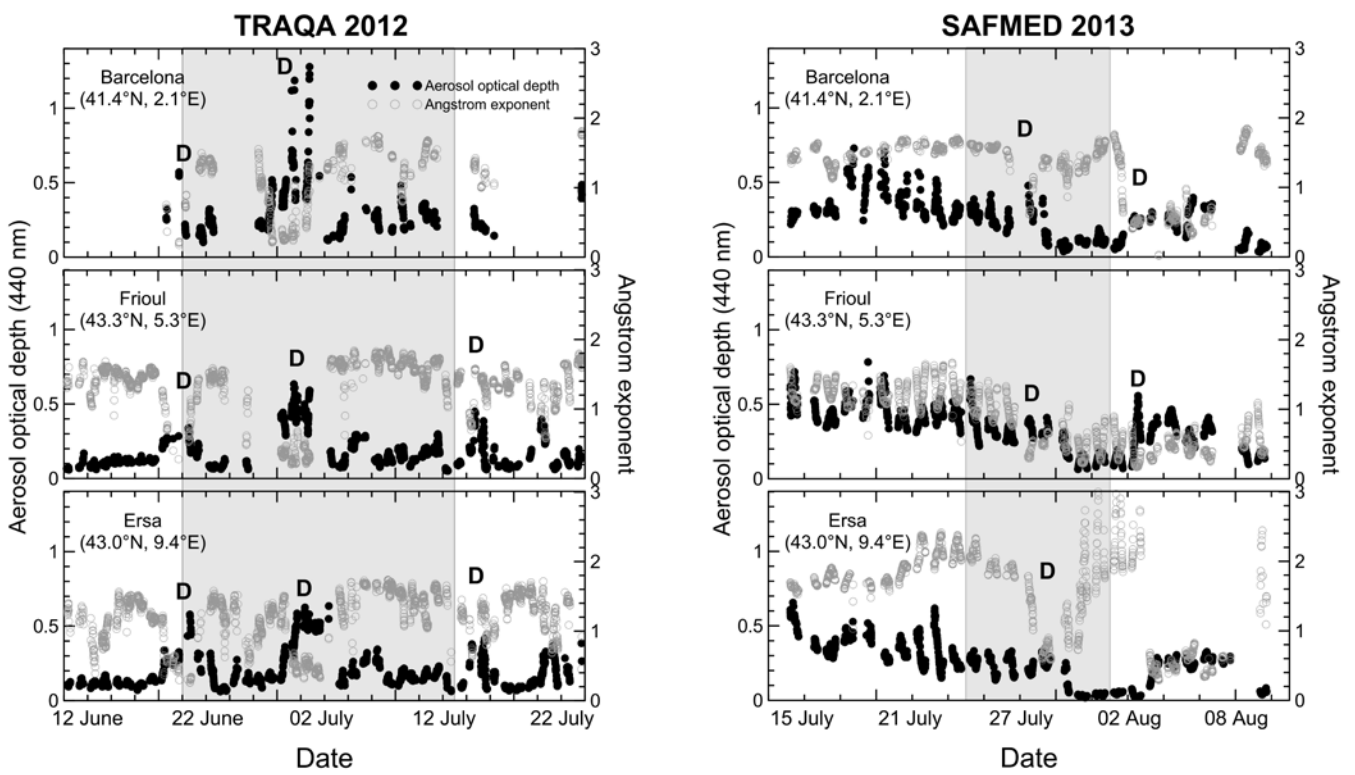
950 **Figure 1.** (Upper panel) Flight trajectories of the TRAQA (20 June - 13 July 2012) and the
951 SAFMED (24 July - 1 August 2013) campaigns. The aircraft was based in Toulouse (43°36'N,
952 1°26'E, France) during TRAQA and in Genoa (44°24'N, 8°55'E, Italy) during SAFMED. (Lower panel)
953 Zoom on the investigated area and geographical position of the different vertical soundings
954 analysed in this paper. The position of the three AERONET stations of Barcelona, Frioul, and Ersa
955 considered in this study is also shown.



958
959
960
961

962
963
964
965
966
967
968
969
970
971
972
973
974
975
976

Figure 2. Aerosol optical depth at 440 nm (τ) and Ångström exponent (α) measured at the Barcelona, Frioul, and Ersa ~~different stations~~ AERONET stations in the Western Mediterranean basin during the TRAQA 2012 (left panels) and the SAFMED 2013 (right panels) campaigns. ~~Data are taken from the stations of Barcelona, Frioul, and Ersa located all around the basin.~~ The time period for the different plots is ± 10 days around the beginning/end of the two campaigns (data for the Barcelona station are not available over the entire period for 2012). The label D indicates the days affected by Saharan dust.

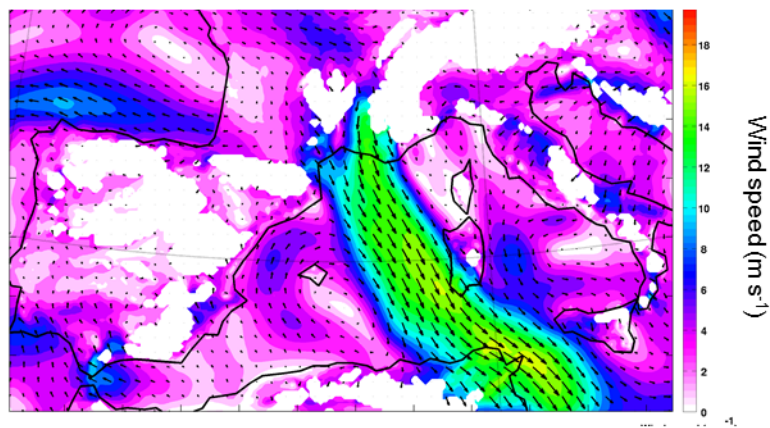


977
978
979
980
981
982
983
984
985
986
987

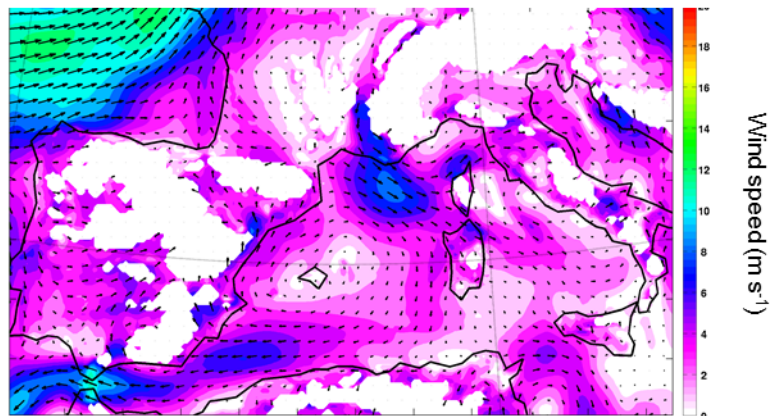
988
989
990
991
992
993
994
995
996

Figure 3. Example of wind maps at 925 mbar for 26 June and 3 July 2012. The maps are obtained from the WRF-Chem model (Weather Research and Forecasting – Chemistry) at 10-km horizontal resolution.

a) 26 June 2012 12UT, 925 hPa



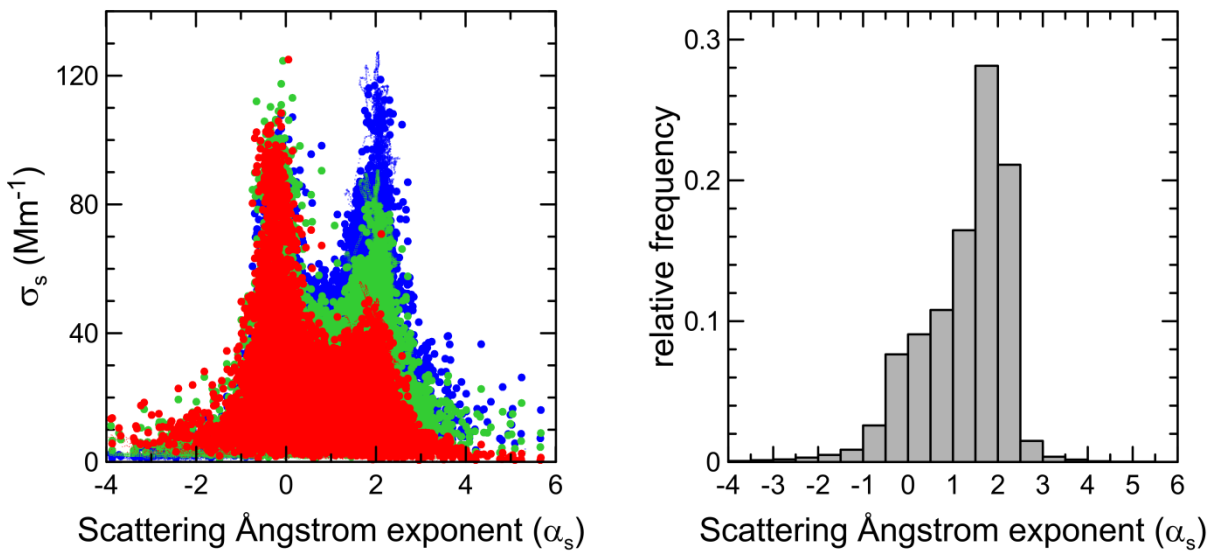
b) 03 July 2012 12UT, 925 hPa



997
998
999
1000
1001
1002
1003

1004
1005
1006
1007
1008
1009
1010
1011
1012
1013
1014

Figure 4. (Left) Scattering coefficient σ_s at 450, 550, and 700 nm versus the scattering Ångstrom exponent α_s . Cases with extremely negative (<-2) and positive (>4) values of α_s are always related with very low scattering coefficients, and are likely due to instrumental noise under low scattering conditions. (Right) Frequency of occurrence of α_s obtained considering vertical profiles data from all TRAQA and SAFMED flights.



1015
1016
1017
1018
1019
1020
1021
1022
1023
1024
1025
1026
1027
1028
1029

1030

1031

1032

1033

1034

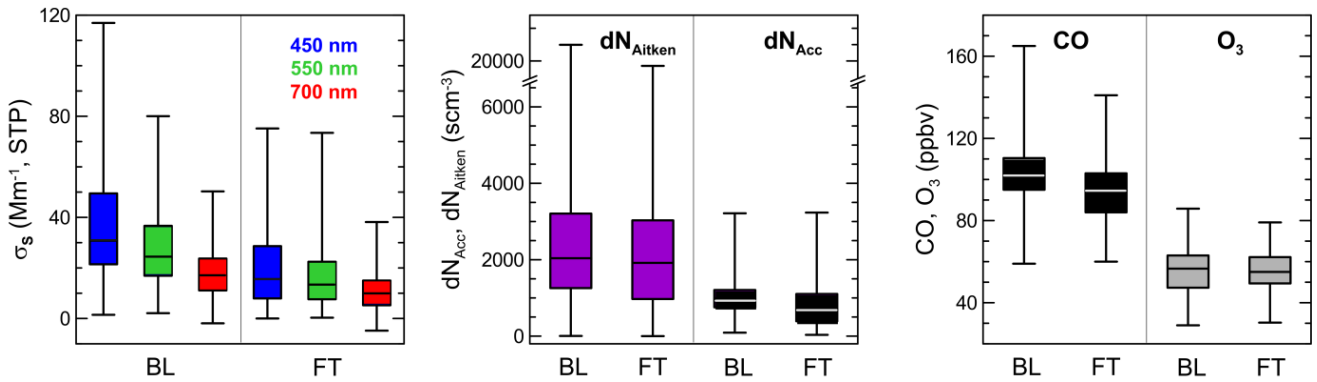
1035

1036

1037

1038

Figure 5. Box and whisker plot of the aerosol scattering coefficient (σ_s) at 450, 550, and 700 nm, particle concentration in the Aitken (dN_{Aitken}) and accumulation (dN_{Acc}) modes, and CO and O₃ measured within pollution plumes in the boundary layer (BL) and in the free troposphere (FT).



1039

1040

1041

1042

1043

1044

1045

1046

1047

1048

1049

1050

1051

1052

1053

1054

1055

1056

1057

1058

1059

1060

1061

1062

1063

1064

1065

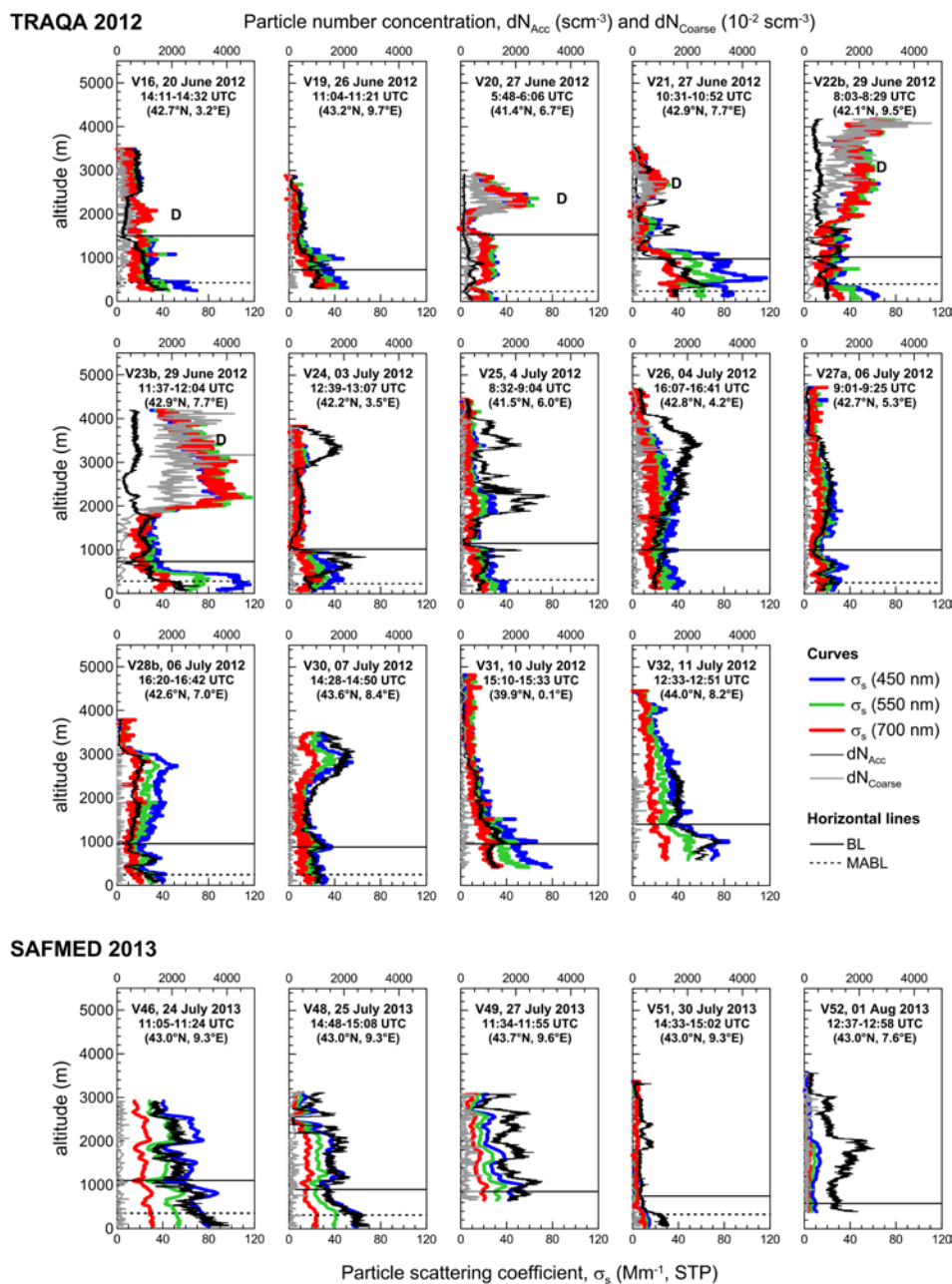
1066

1067

1068

1069
 1070
 1071
 1072
 1073
 1074
 1075
 1076
 1077
 1078
 1079
 1080
 1081
 1082
 1083

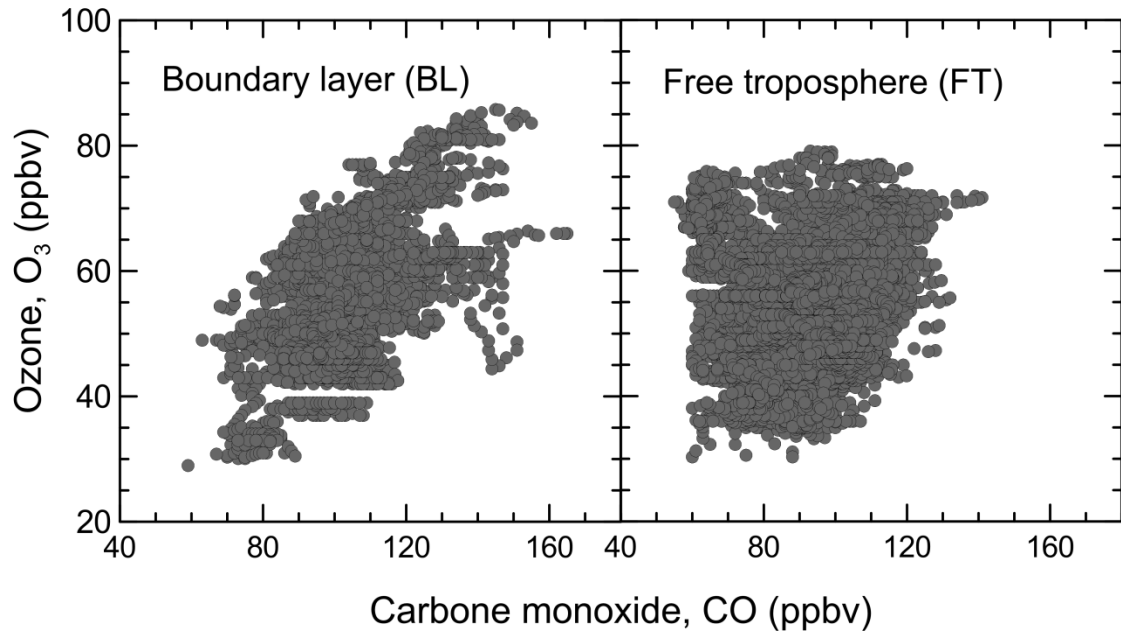
Figure 6. Vertical profiles of the spectral scattering coefficient σ_s at 450, 550, and 700 nm and particle number concentration in the 0.1-1.0 μm (dN_{Acc}) and 1.0-4.0 μm (dN_{Coarse}) diameter ranges observed during TRAQA and SAFMED. Data are reported at STP (standard temperature and pressure, $T = 293.15 \text{ K}$ and $P = 1013.25 \text{ hPa}$). The heights of the top of the marine aerosol boundary layer (MABL) and planetary boundary layer (BL) estimated from the meteorological profiles are also indicated in the plots. The label D is used to identify the aerosol layers affected by Saharan dust. For certain flights (V22, V23, V27, and V28) two vertical soundings were performed; the letters “a” and “b” after the flight number in this plot specify if the considered data are taken from the first or the second sounding, respectively.



1084

1085

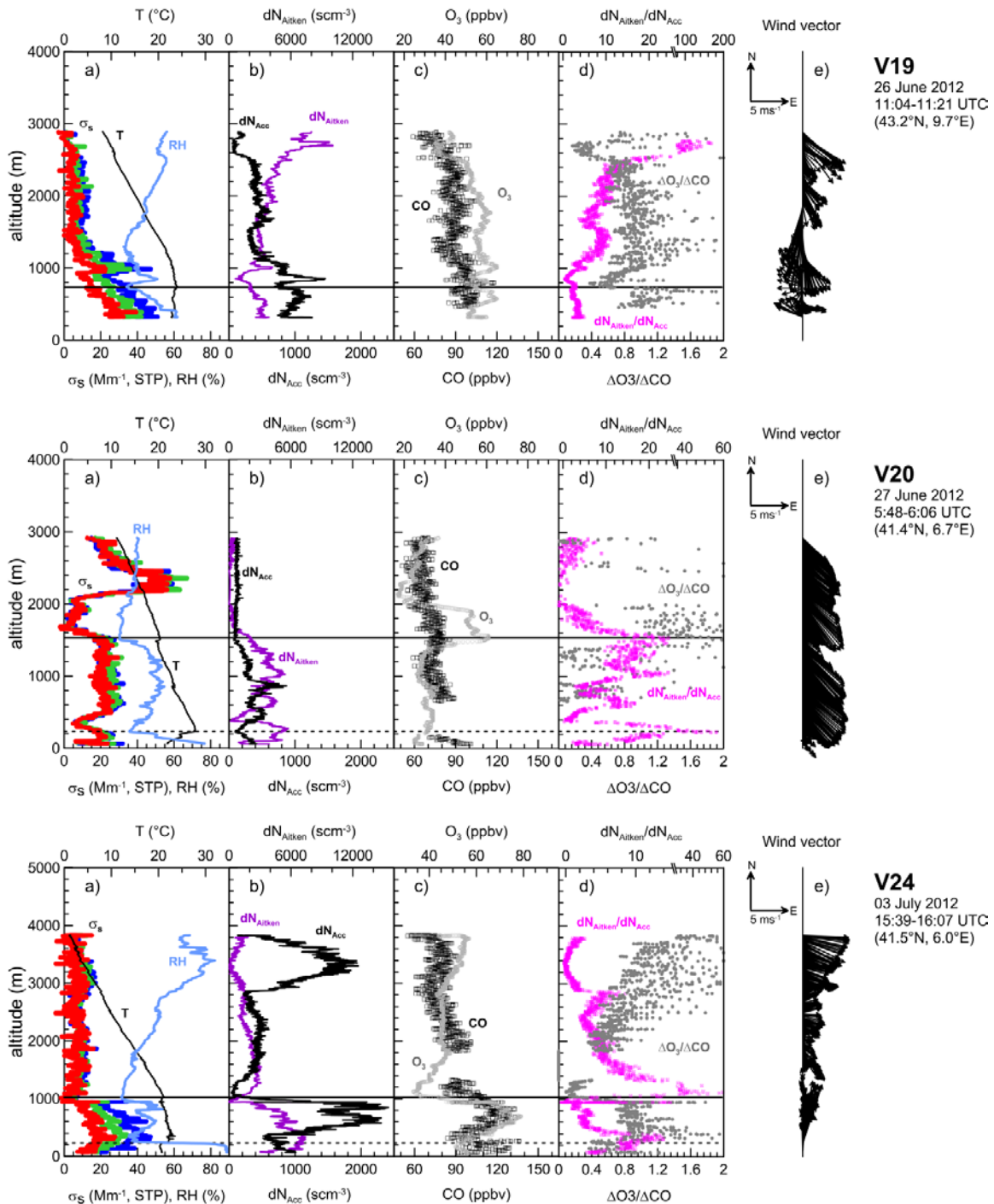
1086 **Figure 7.** O₃ versus CO in the boundary layer (BL) and the free troposphere (FT) for all TRAQA
1087 and SAFMED vertical profiles (dust observations excluded).
1088
1089
1090



1091
1092
1093
1094
1095
1096
1097
1098
1099
1100
1101
1102
1103
1104
1105
1106
1107
1108
1109
1110
1111
1112
1113
1114
1115
1116
1117
1118

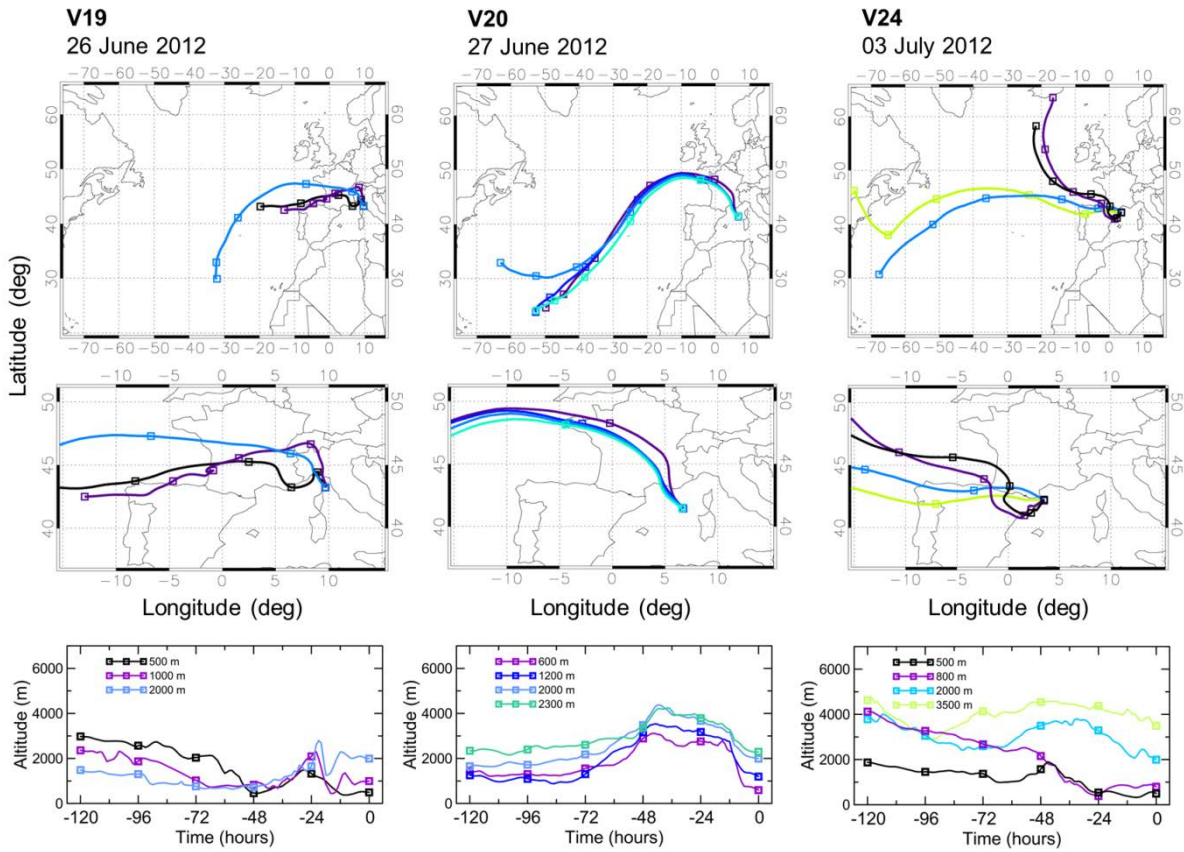
1119
 1120
 1121
 1122
 1123
 1124
 1125
 1126
 1127
 1128
 1129

Figure 8. Aerosol and trace gases vertical profiles for flights V19 (export from northern Italy/Po Valley), V20 (Mistral event), and V24 (export from the Barcelona area). The plots show the: (a) spectral scattering coefficient σ_s at 450, 550, and 700 nm (blue, green, and red lines, respectively), temperature (T, black line), and relative humidity (RH, light blue line); (b) particle number concentration in the 0.004-0.1 μm (dN_{Aitken} , purple line) and 0.1-1.0 μm (dN_{Acc} , black line) diameter ranges, (c) CO (black dots) and O₃ (grey dots) mixing ratios, (d) ozone enhancement factor $\Delta\text{O}_3/\Delta\text{CO}$ (grey dots) and Aitken to accumulation ratio $dN_{\text{Aitken}}/dN_{\text{Acc}}$ (pink dots) and (e) horizontal wind vector. The heights of the top of the MABL (dotted line) and BL (solid line) are also indicated.



1130

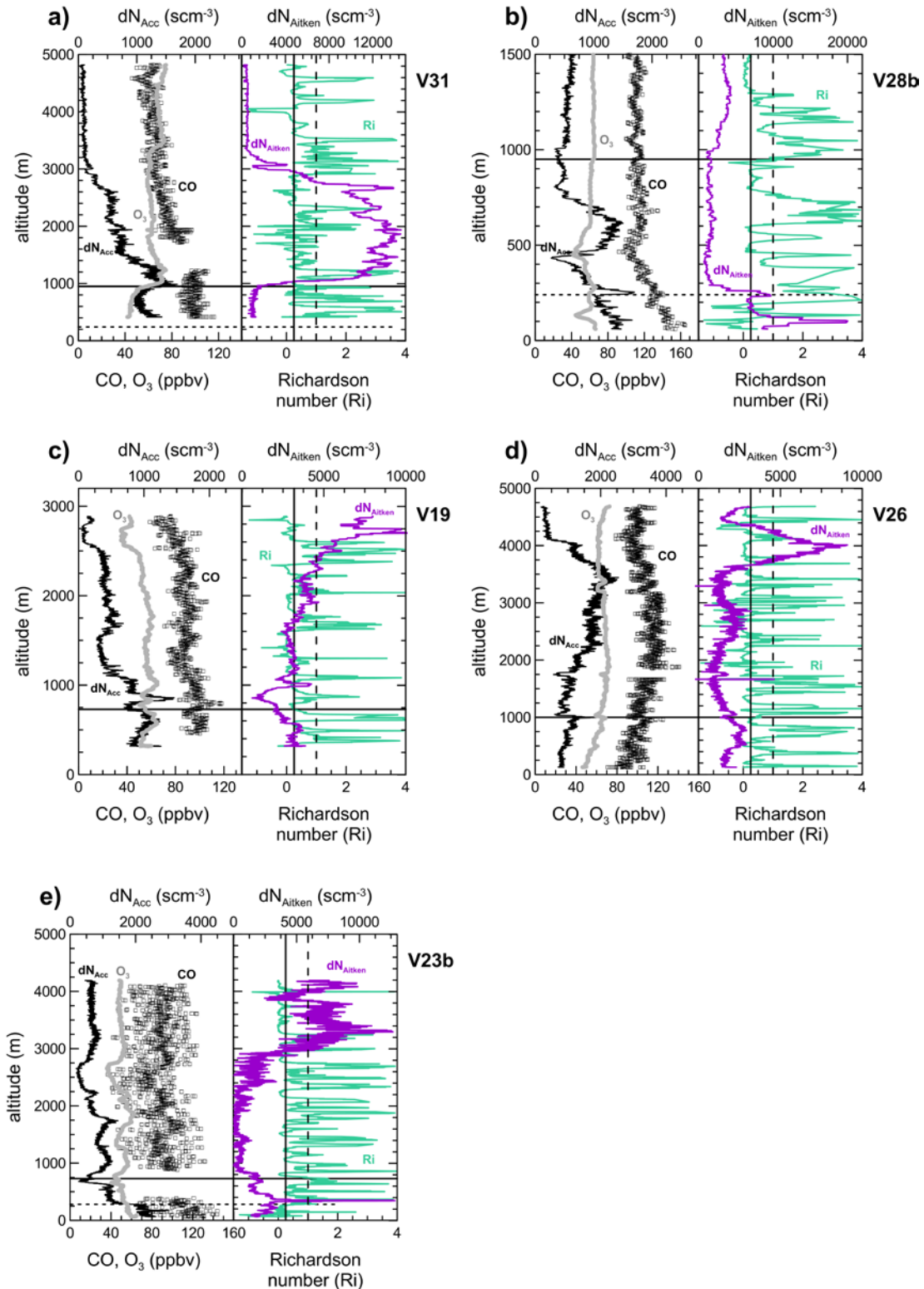
1131 **Figure 9.** Five-days backward air mass trajectories for the V19, V20, and V24 flights calculated
 1132 with the FLEXTRA model. The upper panel shows the trajectories over an extended latitude-
 1133 longitude region, while the central panel zooms on the Western Mediterranean area. The altitude of
 1134 the air masses and its temporal evolution along the five days trajectories is reported in the lower
 1135 panel of each plot.
 1136



1137
 1138
 1139
 1140
 1141
 1142
 1143
 1144
 1145
 1146
 1147
 1148
 1149
 1150

1151
1152
1153
1154
1155
1156
1157

Figure 10. Vertical profiles of the accumulation and Aitken particle concentrations (dN_{Acc} , black line, and dN_{Aitken} , purple line), CO (black dots), O₃ (grey dots), and gradient Richardson number (Ri, green line) for flights a) V31, b) V28, c) V19, d) V26 and e) V23b. The horizontal lines indicate the height of the marine boundary layer MABL (dotted line) and the planetary boundary layer BL (continuous line), while the vertical lines indicate $Ri_{crit}=0.25$ and $Ri=1$ (continuous and dashed lines, respectively).



1158